# Università di Pisa

## Corso di Laurea Magistrale in Ingegneria Biomedica

## Tesi di Laurea:

*"Development of an in vitro biomimetic device aimed at reproducing the intestinal barrier"*

**Candidata**: GIULIA GORI

**Controrelatore**: Arianna Menciassi

**RELATORI:**

Prof. Arti Ahluwalia
Ing. Leonardo Ricotti
Ing. Daniele Cei

ANNO ACCADEMICO 2013 / 2014

**Table of contents**

## MOTIVATIONS OF THE THESIS

The objective of this Thesis is the design, development and characterization of a biomimetic system to be used as a tool to simulate the intestinal barrier *in vitro*.

The *in vitro* mimicking of a biological system allows to establish a model of a phenomenon occurring *in vivo.* This can thus be analyzed singularly and independently from the surrounding environment, which would imply a substantial increase of the parameters to be considered. By using a proper *in vitro* model it is possible to study the response of the system to precise stimuli, thus allowing the prediction of a series of events subsequent to the tuning of certain conditions.

The system proposed in this Thesis is a biohybrid tool, based on a porous polylactid acid nano-membrane, which constitutes the interface between intestinal Caco-2 cells and beating cardiomyocites. The aim is to obtain a chip, useful to test drugs, nanoparticles and other substances, in terms of their toxic and/or therapeutic effects. The work deals with a recent research trend, aimed at engineering on-chip organs and tissues, based in most cases on the coupling of nanostructured materials and cell cultures. These systems are envisaged as tools to complement or to replace tests on animals, widely used at present for toxicological analysis and drugs testing. Worldwide, the estimated number of vertebrates employed for *in vivo* experiments ranges between 10 and 100 millions per year.

In 1959, Russel and Burch proposed the 3R rule, based on the following fundamental principles:

- *Replacement:* replacement of animal testing with alternative methods;
- *Reduction:* reduction of the number of animals employed;
- *Refinement:* improvement of animals living conditions.

The above-mentioned rule was introduced by the European Union, within the 2010/63/UE directive, focused on the safeguard of animals employed for scientific purposes.

From 2009 animal tests were banned in Europe, as a means to test cosmetic products. From 2013, it is also prohibited, in Europe, to sale cosmetic products containg ingredients tested on animals, all over the world.

In addition to ethical concerns, *in vivo* tests are also characterized by long time durations and high costs, thus raising the need of effective alternatives, *in vivo* and *in silico.* The *in vitro* tool developed in this Thesis could be useful for the study of specific diseases related to dysfunctions in intestinal absorption mechanisms. Intestinal malabsorption is a syndrome characterized by an incomplete absorption of nutrients. It can be:

- GENERALIZED: if the absoption dysfunction involves just proteins, sugar and fat and causes diarrhea with fat in the feces;
- SELECTIVE: if the absorption dysfunction involves only one class of nutrients;
- TOTAL: it the absorption dysfunction involves the whole small intestine and always causes diarrhea;
- PARTIAL: if the absorption dysfunction involves only a specific intestinal tract and it does not cause diarrhea.

Intestinal absorption dysfunctions can also be incidental to diseases of other organs such as the exocrin pancreas. It is possible to discriminate among the following cases:

- absorption dysfunction caused by a predominant endoluminal deficiency: of pancreatic origin (chronic pancreatitis, pancreas cancer, cystic fibrosis); of biliary origin and due to enzyme inactivation;
- absorption dysfunction derived from a predominant parietal defect: celiac disease, Crohn's disease, amyloidosis etc. The absorption insufficiency can arise from a reduction of the available absorption surface (in case of extended resection), from an altered absorption

surface (celiac disease, Crohn's disease), from unsufficient blood supply, from lymph outflow obstructed in its path and from intracellular transport selective defects.

Taking into account these considerations, the purpose of this work arises from the need to have a tool that allows to model the physiological and pathological features of intestinal barrier and, on the other hand, of the absorption mechanisms through it. A commonly accepted intestinal absorption model consists of a layer of Caco-2 cells, extracted from the human colon and cultured on a polycarbonate membrane, within a transwell**.** In this system, the substances to be tested are provided in correspondence of the apical side of the monolayer and the compounds filtered through the cells are monitored in correspondence of the basolateral side. The traditional model has some limitations, in terms of the expression of particular proteins, of cellular morphology, but above all for the lack of peristalsis, which implies an altered permeability. Taking into account the intrinsic limitations of the traditional models and the lack of suitable technologies and procedures in the state of the art, this work aims at:

**• developing a ultra-thin polymeric membrane provided with highly regular pores (conferring high permeability to the system) and showing high biocompatibility, thus allowing the culture of intestinal Caco-2 cells and cardiomyocytes. This will allow, with few evolutions of the device, to replace monocultures with co-cultures of these cells;**

**• developing a biohybrid tool that would be able, in future evolutions of the system, to generate contractile movements which simulate *in vitro* the peristalsis of the intestine occurring *in vivo*.**

The Thesis is based on a multidisciplinary research effort, combining know-how and technologies typical of different fields, such as materials science, molecular biology and micro-/nano-fabrication. It represents properly the interdisciplinarity that is typical of the bioengineering field, aiming at developing innovative systems for diagnosis and therapy.

# 1. INTRODUCTION

## 1.1 INTESTINE ANATOMY AND PHYSIOLOGY:

Before specifically describing intestine, an overview of the whole apparatus it belongs to and a sketch of its functions are desirable. The attention was focused on those functions accomplished by the organ and targeted by the *in vitro* model proposed. In this Thesis, the digestive apparatus, which includes also the intestinal tract, accomplishes the following key processes **[16]:**

- **DIGESTION:** chemical and mechanical fragmentation of food in smaller units, able to pass through the intestinal epithelium and thus to enter into the organism.
- **ABSORPTION:** either active or passive transport of substances from the lumen of the gastro-intestinal tract to the extracellular fluid.
- **MOTILITY:** muscular contraction, causing the movement of substances along the gastrointestinal tract. This movement has to guarantee an advancement of food within the intestinal lumen lasting a time interval sufficient to allow the digestion of nutritious substances and promotes simultaneously their absorption through the intestinal barrier.
- **SECRETION:** transport of water and ions from the extracellular fluid to gastrointestinal lumen, and secretion of substances from the cells of the digestive canal. The secretion is controlled in order to guarantee the supply of proper quantities of digestive enzymes, so that the food within the gastrointestinal tract can be fragmented in absorbable forms.

## 1.1.1 DESCRIPTION OF THE INTESTINAL TRACT:

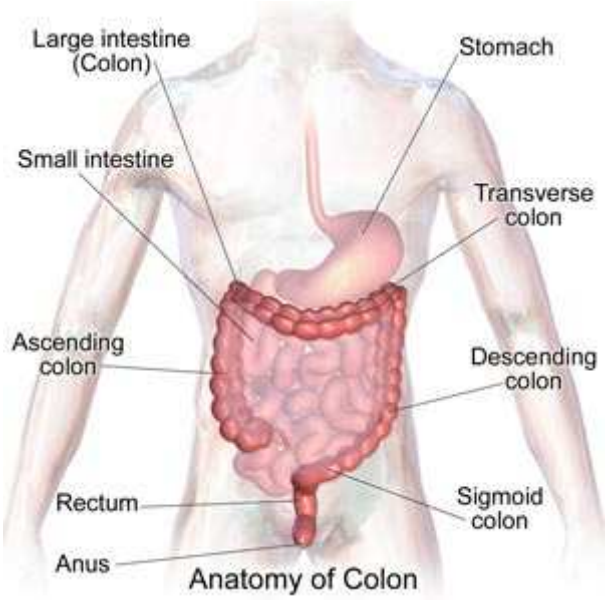


*Figure 1.1: Depiction of the intestine components: small intestine, large intestine, rectum and colon.*

The small intestine is conventionally divided into three parts: duodenum, jejenum and ileum (jejenum and ileum constitute the mesenteric part). They are located in the abdominal cavity and the blood vessels, connecting the small intestine to the rest of the body, go through the mesentery. Figure 1.1 depicts the overall intestine structure, involving small intestine, large intestine, rectum, colon and anus.

The small intestine is composed of four concentric tunicae, as shown in Figure 1.2 and Figure 1.3.

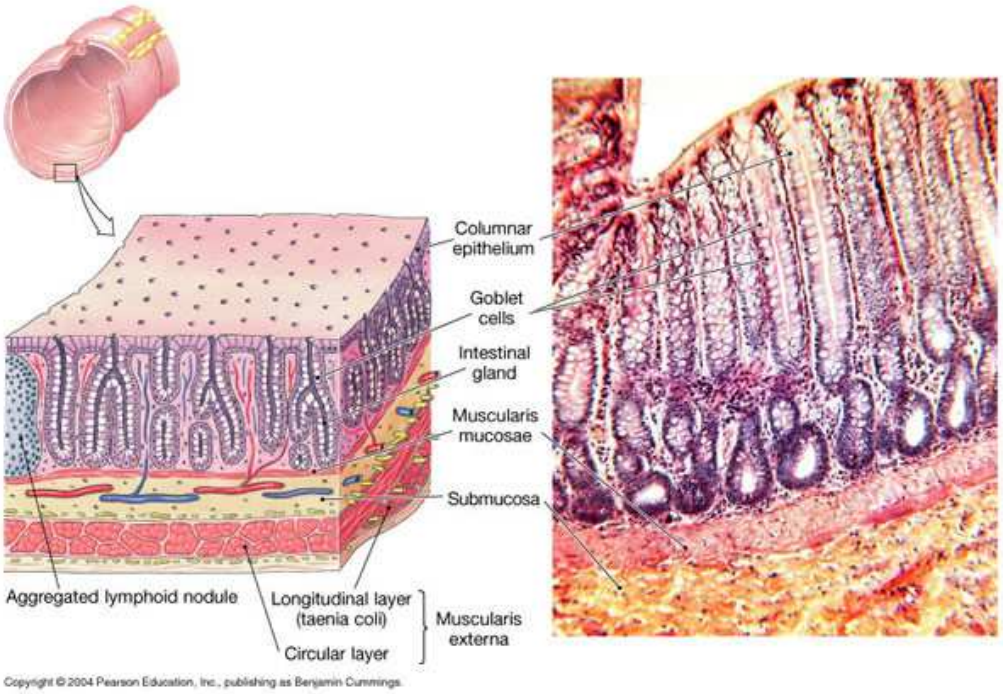


*Figure 1.2: Small intestine structure.*

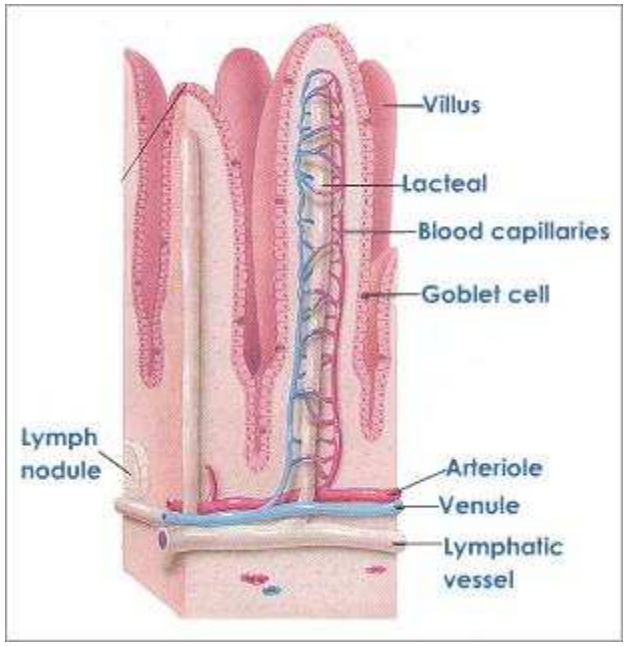


*Figure 1.3: Small intestine structure, showing a surface topography characterized by crypts and villi.*

The tunicae are the following:

- TUNICA SEROSA: constituted by the peritoneum (a layer of flat endothelial cells that lay on an well-grown elastic membrane) and the underlying subserosa (thin layer of

connective and adipose tissue containing blood and lymph vessels).

- TUNICA MUSCULARIS: consisting of two layers of smooth muscle cells: an external longitudinally oriented one and an internal (thicker) circularly oriented one.
- TUNICA SUBMUCOSA: composed of connective tissue, which is very rich of blood and lymph vessels.
- TUNICA MUCOSA: characterized by three layers. From the external to the internal side, they are:

- *Muscolaris mucosae:* thin layer of smooth muscle cells, mainly longitudinally oriented. Intestinal villi emerge from this layer.

- *Lamina propria:* it constitutes the villus axis; it brings in the villus the vascular structures and the thin muscle fibers that allow villus contraction.

- *Epithelial layer:* villus lining layer.

Intestinal villi are protrusions that extend perpendicularly to the small intestine mucosa, thus confering it a velvety aspect. Villi are characterized by heights ranging between 320 and 570 µm and thicknesses of about 85-140 µm. Microvilli rise perpendicularly from the villi tips and they reach a maximum height of about 1.3 µm and thicknesses of about 0.2 µm. Microvilli increase the intestinal absorbing surface of about 20 times. The typical structure of the intestinal barrier, formed of superficial projections (villi and microvilli) is shown in Figure 1.4.

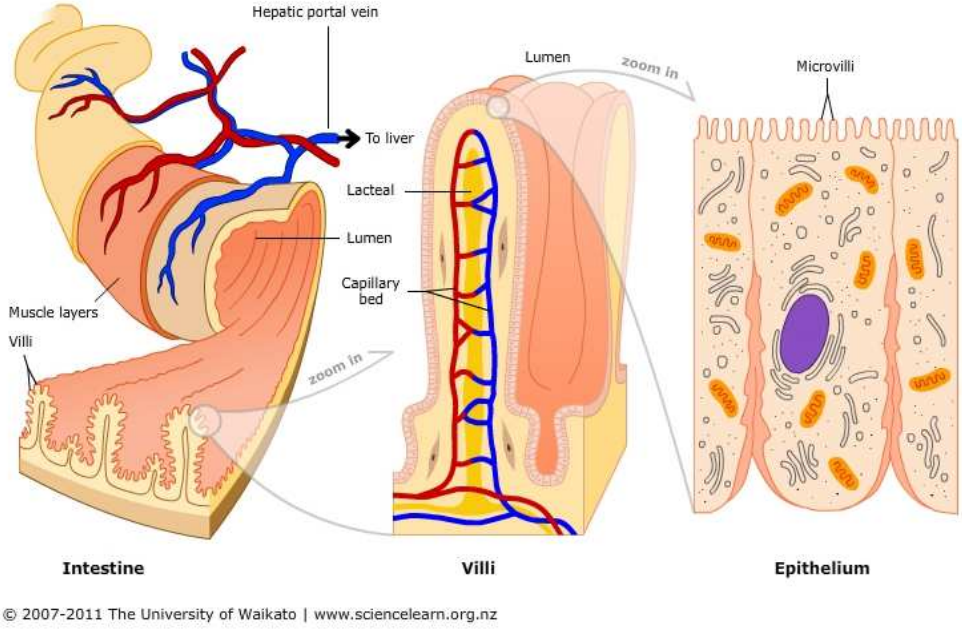


*Figure 1.4: Intestine superficial protrusions (villi and microvilli) that increase the absorption of substances through the intestinal barrier.*

An important characteristic, which allows the transit of bio-compounds within the gastrointestinal tract (GI) is the intestinal motility. Ater its evacuation from the stomach, the chyme enters in the small intestine and it is pushed ahead through the duodenum. Muscle twitches allow chyme mixing with enzymes and its exposure to the absorbing mucosa. The two main types of intestinal motility are:

***Segmenting contractions:*** localized contractions, involving the whole circumference of the small intestine muscular tunica and lasting a few seconds. The contractions take in the lumen and tend to divide its contents. In general they are stationary and localized in a specific intestinal tract, but they could also be propellant and continuing for some centimeters. Segmenting contractions constitute the most common type of intestinal motility. It is possible to distinguish *simple segmenting contractions,* characterized by an irregular pattern, and *rhythmic segmenting contractions.*

***Peristaltic contractions:*** they have a length of about 4-5 cm and they propagate along a short tract of the intestinal loop with a speed of 1-2 cm per minute. The speed is higher within the duodenum and it decreases within the ileum. Peristaltic contractions allow the movement of intestinal contents towards the distal intestinal parts. Peristalsis is a traveling contraction wave produced by the contraction of circular muscles upline, the contraction of longitudinal musculature and, parallely, the relaxation of the circular musculature downstream respect to the stimulation location.

Figure 1.5 illustrates the difference between the segmenting and the peristaltic contractions, previously described.

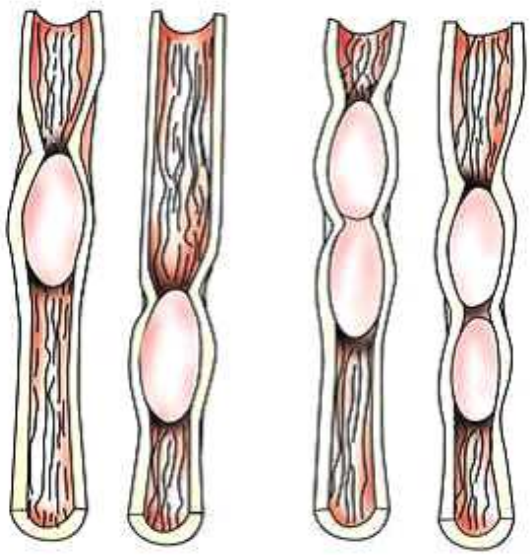

*Figure 1.5: Representation of the two types of intestinal motility: peristaltic (on the left) and segmenting contractions (on the right).*

It is necessary to guarantee a sufficiently slow progression of the chyme along the intestine, in order to allow the proper absorption through the intestinal barrier. The small intestine receives an average of 5.5 liters of food, liquids and secretions and approximately other 3.5 liters of hepatic, pancreatic

and intestinal secretions. The total volume of the intestinal lumen is about 9 liters per day. In a day additional secretions involve:

- **BICARBONATE**: it originates mainly from pancreas; it neutralises the chyme (very acidic) which reaches the small intestine from the stomach;
- **BILE**: bile salts are essential for fat digestion;
- **MUCUS:** secreted by intestinal goblet cells, with a function of protection and lubrication;
- **DIGESTIVE ENZYMES**.

Most of the ingoing liquids (about 7.5 liters respect to the 9 liters input initially) are reabsorbed by the intestine. Organic nutritious substances and ion transport, which take place mainly in the duodenum and in the jejenum, create an osmotic gradient that causes the resulting absorption of water. Most of the nutritious substances absorbed enters in intestinal villi capillaries and then in the hepatic portal system. The small intestine represents the location where the main part of the digestion takes place. The junction between small intestine and colon acts as a sphincter, thus regulating the flux of substances from the ileum to the caecum and preventing retrograde transport. The sphincter opens when the peristaltic wave, which passes along the ileum terminal part, generates a pressure that is sufficient to overcome the sphincter resistance. The colon starts in correspondance of the ileum-caecum sphinter and it stops in the rectum (Figure 1.6).

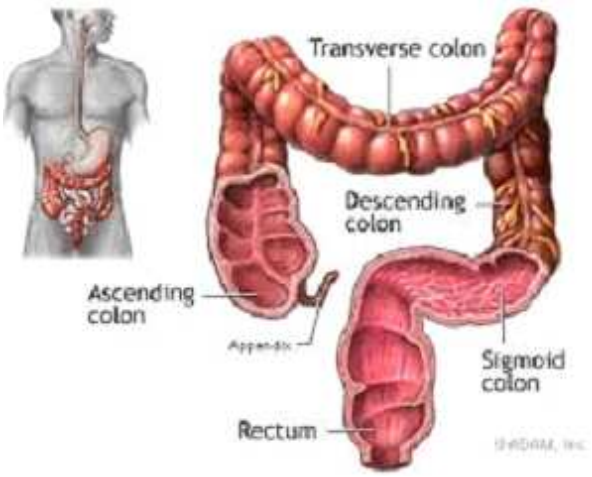


*Figure 1.6: Large intestine components.*

The intestinal barrier (**[17]**) is the functional unit that guarantees the stable balance between the antigen charge of intestinal lumen and the complex immunologic and non immunologic organization of the intestinal mucosa. The intestinal barrier accomplishes two key functions for the survival of individuals: it allows the absorption of nutritious substances and drugs and it defends the organism from penetration of damaging macromolecules. Intestinal flora, mucous layer, intestinal epithelium, natural and acquired immunity components, endocrine system, vascular lymphatic system and digestive enzymes are essential factors for a proper functioning of the intestinal barrier. All of these components are characterized by mutual complex interactions, which allow to preserve intestinal barrier capability to prevent systemic transport of damaging substances.

## 1.1.2 ABSORPTION MECHANISMS OF DRUGS AND NUTRITIOUS SUBSTANCES:

The main functions of intestine are digestion and absorption of drugs and nutritious substances. They actually pass through the intestinal barrier, acting as a selective porous membrane. Intestinal absorption represents the last digestive phase. It determines the transport in the blood flow,

through the intestinal walls, of substances obtained from the digestion of macromolecules contained in the food. These substances are: mainly glucose (derived from starch and saccharose), amino acids (derived from proteins), glycerol and fatty acids (derived from fats), vitamines and salts. Most of the absorption takes place through the jejenum and the ileum walls. Small intestine walls are shaped in several folded structures covered with thousands of thin projections, called intestinal villi. Each villus is 1 mm long and there are about 3000 villi for each cm square. The surface of each villus is further increased by the presence of microvilli, produced by superficial protrusions of the intestinal villi cladding membrane. The intestine internal surface is characterized by a topography with a crypt-villus pattern. This feature promotes intestinal absorption and it is responsible of the transport of bio-compouds.

In correspondence of the crypts, secretion of substances mainly takes place, whereas villi are specialized structures responsible for intestinal absorption, as they increase the transport and absorption surface available. Molecules pass through microvilli membranes. Each villus is formed of a capillary network, in which blood flows. Glucose, amino acids, salts and vitamines are filtered and transported into the blood. Intestinal capillaries converge in a blood vessel, the *portal hepatic vein,* which enters into the liver. Figure 1.7 depicts the intestinal barrier surface structure, constituted by crypts and villi.

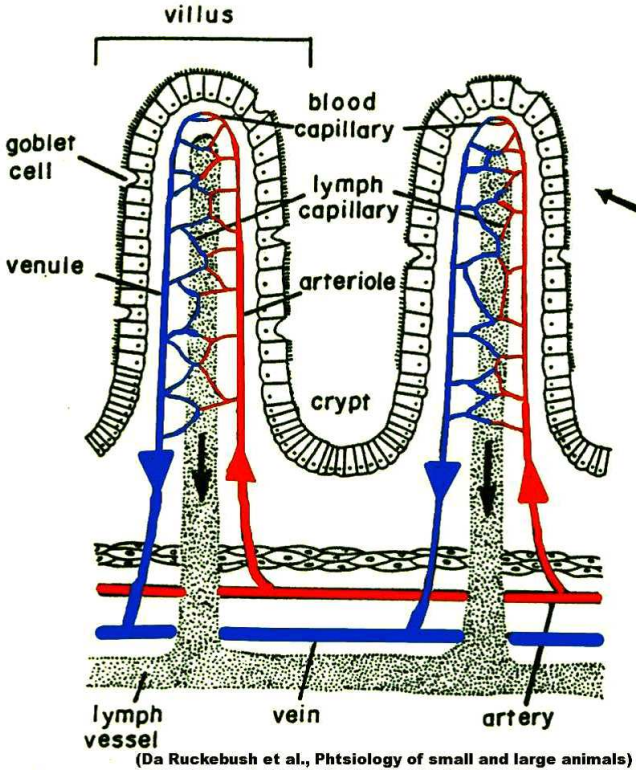


*Figure 1.7: Intestinal surface topography characterized by crypts and villi.*

Fats follow a different metabolic path. After going though the microvilli membrane, glycerol and fatty cluster, reconstituting triglycerides and they are conveyed in lymph vessels. Lymph vessels then flow into a single conduct that flows into the circulatory stream. All of the molecules, which derive from food digestion are thus released directly or undirectly in the blood. After a first absorption in the small intestine, substances continue their path within the large intestine. Here, mucosa glands secrete only mucus and not enzymes. Even if the walls are oiled by the mucus, the transit time of intestinal contents is rather long: it ranges between 2 and 6-7 hours. In large intestine water and mineral salts are absorbed and food which was not digested is eliminated with the faeces. Nutritious substances, mineral salts and vitamines are absorbed through the intestinal barrier thanks to one or more active transport mechanisms. They are energy-dependent transport processes mediated by membrane proteins and they work either against concentration gradient or in absence of electrochemical concentration gradient. Intestinal epithelial cells are key mediators for water and ions absorption. Macrophages, muscle cells and enteric nervous cells interact with them.

Fat assimilation needs integrated processes involving the digestive phase, the following absorption phase and the post-absorption phase. Carbohydrates instead, are absorbed only in the small intestine in form of monosaccharides. Their absorption requires the presence of a sodium pump and of a "carrier protein". Before their absorption they are digested by two enzymes involved in the process: pancreatic amylase and intestinal disaccharidase. Protein absorption instead requires an extensive hydrolysis phase aimed at reducing them in form of di- or tri- peptides or simple amino-acids. Proteolysis is carried out in the stomach and in the small intestine mainly thanks to two enzymes: trypsin and pepsin. Figure 1.8 depicts the main routes of bio-compounds absorption through the intestinal barrier.

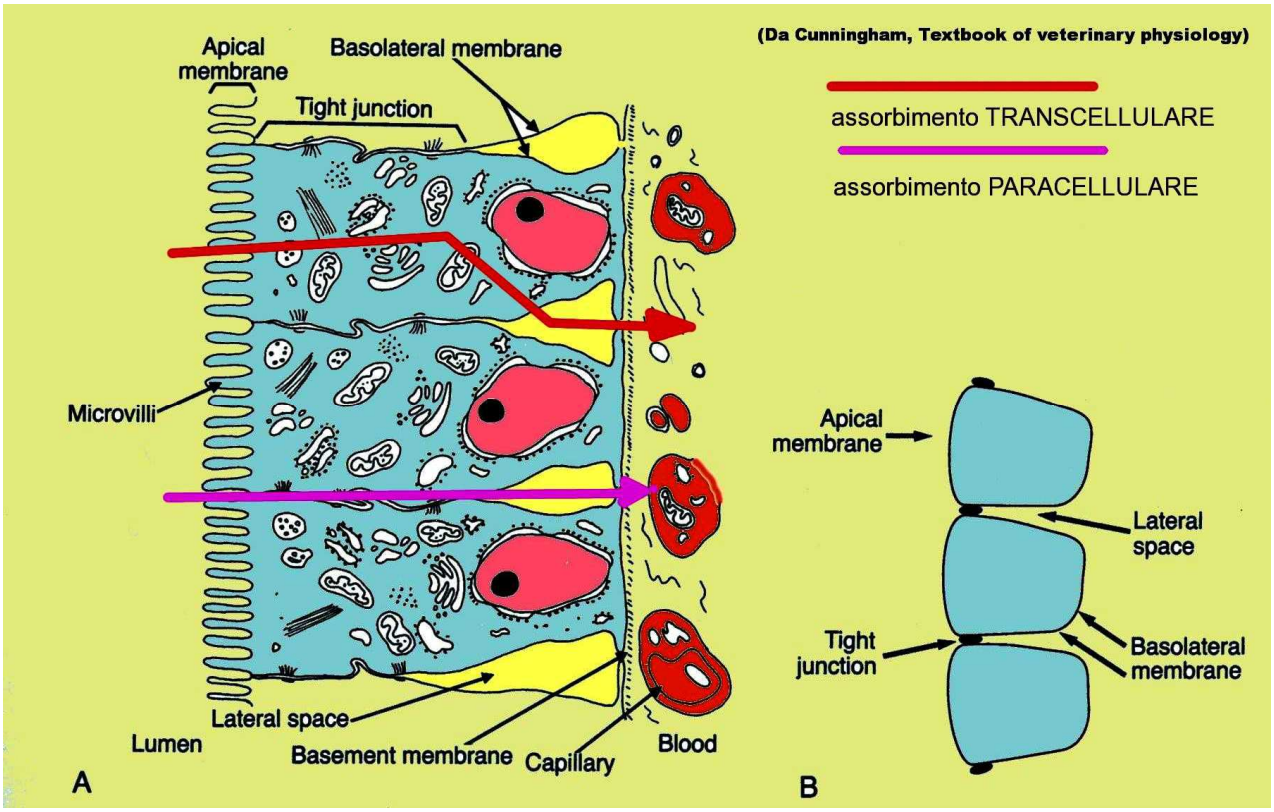


*Figure 1.8: Representation of the absorption routes of absorption through the intestinal barrier.*

Concerning drug absorption, there are different routes, which can be distinguished between entheral and parentheral ones. In the case of entheral assumption (enteron is the latin word for intestine), the drug is in contact with the digestive channel mucosa, whereas in the case of parentheral assumption the drug enters the organism by injection. In relation to the aim of this work, we focus mainly on the entheral route. Drug absorbtion is the transport mechanism of the drug from its administration site to the circulatory stream. Its speed and efficiency depend on the administration route. The intestinal epithelium acts as a selectively permeable barrier, through the formation of complex protein-protein networks that mechanically link adjacent cells and seal the intercellular space. The protein networks connecting epithelial cells form three adhesive complexes: desmosomes, adherens junctions, and tight junctions. These complexes consist of transmembrane proteins that interact extracellularly with adjacent cells and intracellularly with adaptor proteins that link to the cytoskeleton **[46].** The predominant cell type in all absorbing regions is referred to as an enterocyte. Enterocytes are columnar epithelial cells that are bound to their neighboring cells at the luminal surface by tight junctions. Their apical cell membranes posses numerous microvilli which greatly increase the surface area available for absorption **[47].** At various portions of the absorbing regions, absorption is favored by mucosal structures such as fenestrations (small holes) in the endothelial cells of the capillaries, or pores of different sizes in the membranes of the enterocytes. Underlying the lamina propria is a thin layer of smooth muscle, the muscolaris mucosae. In regions of active absorption such as the small intestine, the muscular layer appears to be related to the rhythmic movements of the villi that agitate the layer of intestinal secretions and chyme that are in contact with the epithelium and thus promote absorption.

Figure 1.9 summarizes the different mechanisms of transport through intestinal barrier.

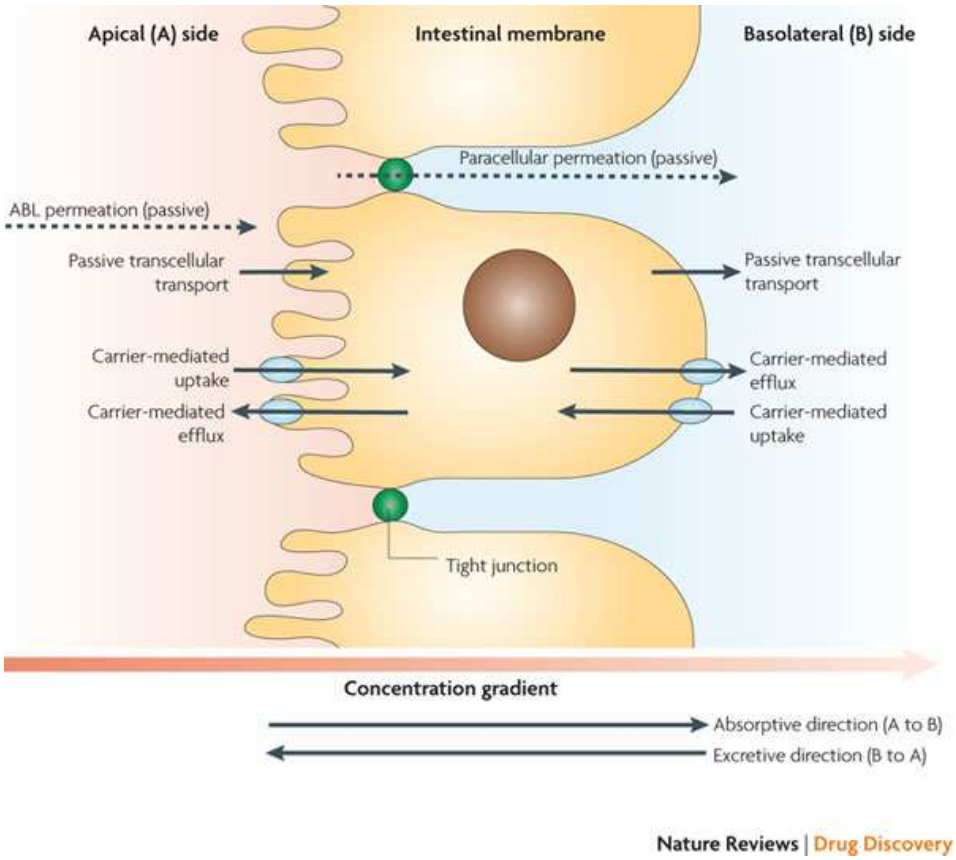


*Figure 1.9: Representation of the different transport routes of drugs.*

Drug transport can be based on one of the following processes:

*PASSIVE DIFFUSION:* according to concentration gradient or electrochemical gradient;

*SPECIALIZED TRANSPORT:*

*FACILITATED DIFFUSION:* water-soluble drugs with molecular diameter higher than 4 Å pass through the fat layer by means of carriers (as depicted in Figure 1.10);

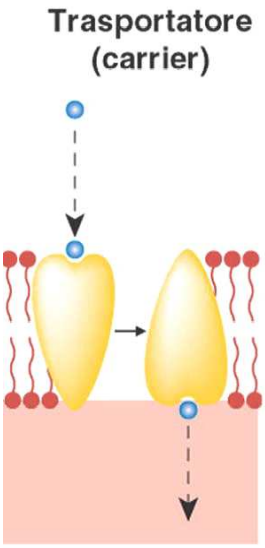


*Figure 1.10: Transport mediated by carriers.*

*ACTIVE TRANSPORT:* requires energy consumption (ATP).

*ENDOCYTOSIS-PHAGOCYTOSIS:* water-soluble drugs characterized by large diameters enter the cell by invagination of the cellular membrane and further formation of vescicles (Figure 1.11).

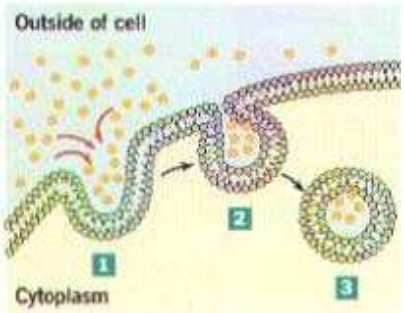


*Figure 1.11: Transport by endocytosis.*

*FILTRATION:* drugs pass through the intercellular spaces of capillaries endothelium according to

pressure gradient and molecular diameter, independently from their fat solubility, polarity and percentage of ionization.

Most of drugs are absorbed by passive diffusion in their non ionized form. The percentage of the available non ionized drug amount depends on two aspects: on the one hand it depends on environmental pH, on the other hand it depends on its pKa. pKa is the dissociation costant, which refers to the amount of dissociated molecules. In particular it represents the pH that determines 50% of the molecules dissolved to be in the ionized form. Drugs are shared by the three components of the organism: blood, extracellular fluid and intracellular fluid. The amount of drug in each of the components depends on their physical and chemical properties. In particular, drug absorption is determined by the following causes:

- **Mass action law**: according to the theory, a great number of small particles (in particular atoms and molecules), even if they are individually characterized by random motion, can be attributed to a higher-level model. The resulting overall movement is in fact directional. The mass action law states that the speed of a chemical reaction is proportional to the concentration of the substances involved. The variation of the amount of products obtained is then proportional to the product of reagents activities.

- **Henderson-Hasselbach equation**: it describes the derivation of pH as a measure of acidity in biological and chemical systems. In fact it represents the relation between pH and acid concentration by the use of its pKa (negative logarithm of its acid dissociation constant).

- **Pharmaceutical stage** (characterized by the capability of the drug pharmaceutical form to release the active principle, which has to be absorbed and submitted to pharmacokinetic processes)**;**

- **Particles dimensions** (the process of particles absorption is faster or slower according to the dimensions of the particles)

- **Gastrointestinal pH and resistance to gastric pH**;
- **Absorbing superficial area;**
- **Speed of blood flow;**
- **Physical and chemical interactions with intestinal contents, resistance to stomach, intestine and intestinal flora enzymes**;
- **Gastrointestinal motility;**
- **Specialized transport;**
- **Enterohepatic circle;**

Drugs, which show low solubility in fats, are in general scarcely absorbed by the intestine. However, some drugs are absorbed thanks to transport systems based on carrier proteins. Drug absorption physiology in the gastrointestinal tract affects the bio-availability of the drug, namely the drug fraction entering the systemic circulation.

## 1.1.3 INTESTINAL MALABSORPTION DISEASES:

The *in vitro* model proposed in this thesis is conceived as a tool aimed at simulating the intestinal barrier, both as a permeable route of transport of bio-compounds and drugs, and in terms of its physio-pathological features and functioning in the case of malabsorption diseases. In fact, the physio-pathological *in vitro* model proposed is conceived as a useful tool to study malabsorption pathologies in terms of their dynamic development and characteristic features, in order to allow the development and the optimization of pharmacological focused effects.

Malabsorption through intestinal barrier can originate from various diseases or their consequences. The mechanism can be represented either by a direct alteration of the intestinal absorption or by digestive dysfunctions that are responsible of the altered absorption. In succession there are some

examples of symptoms typical of intestinal malabsorption diseases. Malabsorption symptoms are caused by the effects of osmotically active substances within the GI tract or by nutrient deficencies that this condition implies. The symptoms are weight loss, wrist-breech spasms, absence of tendinous reflexes, cutaneous ecchymosis, flatulence, abdominous spread and problems due to the increase of the intestinal mass and to gas production. Secondary nutrient deficits, instead, arise proportionally to the severity of the primary disease and they depend on the specific area of the GI tract affected. Many patients affected by malabsorption are often anaemic, normally because of iron deficiencies. Iron deficit arises usually in the case of celiac disease and of gastrectomy. Malabsorption diagnosis is mainly based on fecal fats measurements; it represents the most reliable test allowing a credible diagnosis. Other diagnostic evaluations are based on faeces inspection and faeces microscopic exam. The faeces, in fact in the case of intestinal malabsorption pathologies, are characterized by a typical well-identifiable appearence: for example the presence of not digested food fragments suggests either extreme intestinal ipermotility or short intestine syndrome. Another useful screening method is based on absorption tests. For example, d-xylose absorption test represents an indirect bur rather specific measurement method of the absorption through small intestine proximal part. Small intestine biopsy furthermore at the jejenum level is a routine procedure that allows to extract jejenum succus, which is then subjected to a microbiological analysis of intestinal flora. Endoscopic biopsies are also very useful, if executed in the second segmentum of the duodenum. Duodenum histologic analysis allows specific diagnosis of various intestinal malabsorption diseases, in particular concerning the celiac disease, white diarrhoea and herpetiformis dermatitis, characterized by intestinal villi atrophy. Intestinal malabsorption can be:

- **GENERALIZED**: in this case it regards proteins, sugar and fats and it causes diarrhoea and fat within the faeces;
- **SELECTIVE:** in this case it regards a single class of nutritious substances;
- **TOTAL:** in this case it regards the entire small intestine and it always causes diarrhoea;

- **PARTIAL**: in this case it regards a single intestinal tract;

It is possible to discriminate also between:

- MALABSORPTION DUE MAINLY TO ENDOLUMINAL DEFICIENCIES: it can be of pancreatic origin, of bilious origin and it could be also due to enzymatic inactivation;
- MALABSORPTION DUE MAINLY TO PARIETAL DEFICIENCIES: celiac disease, Crohn's disease, lymphoma, amyloidosis etc. Intestinal absorption inadequacy can derive from a reduction of the absorption surface (extended resections), from alterations of the absorption surface (celiac disease, Crohn's disease, lymphoma), from insufficient blood supply, from lymph obstructed flow path and from intracellular transport selective deficiencies.

Intestinal malabsorption diseases, as in the case of celiac disease, are supposed to be also of genetic origin. Malabsorption causes and the responsible genes are still under investigation, there are in fact many research efforts aimed at discovering the disease-causing factors, not fully understood so far.

Malabsorption is a term that refers to the following features:

- inadequate food digestion;
- insufficient nutrients absorption through intestinal cells;
- alteration of nutrients transport along lymphatic vessels.

Malabsorption causes derive mainly from the reduction of enzymes that are necessary to guarantee food digestion and absorption. Below some diseases that cause dysfunctions of the absorption mechanisms through the intestinal barrier are described.

Celiac disease is an autoimmune, multi-organ disease, characterized by the production of auto-antibodies and by the appearing of intestinal damages caused by gluten ingestion in individuals with genetic alterations. The celiac patient is characterized by a total and permanent intolerance towards

gluten, a protein contained in many kinds of food. Gluten determines intestinal mucosa atrophy and it can cause also Durhing herpetiformis dermatitis consisting of cutaneous lesions in correspondance of limbs, trunk, glutei and head. Figure 1.12 below depicts the difference in the appeareance of intestinal mucosa in the case of a healthy individual and in the case of a celiac one. The celiac individual is characterized by an evident villi atrophy.

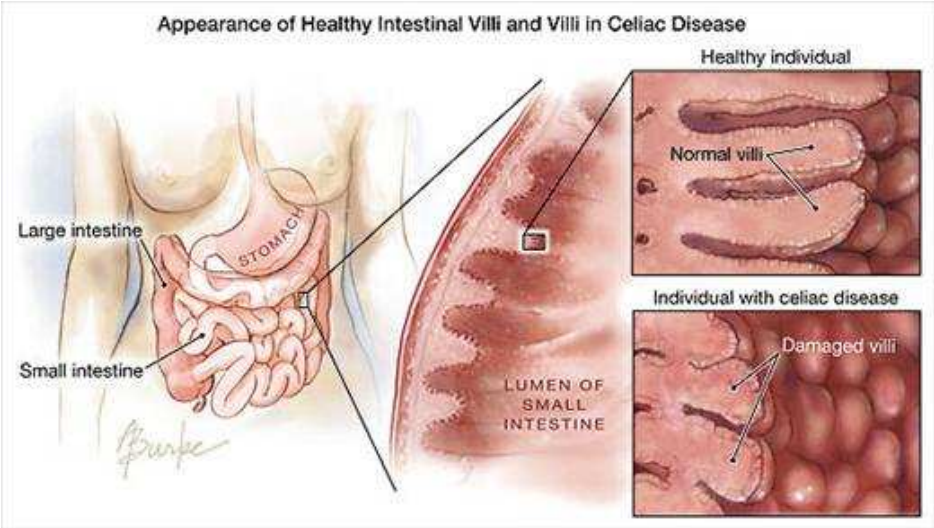


*Figure 1.12: Comparison between the appeareance of intestinal mucosa in the case of an individual which is not affected by intestinal malabsorption (left), and in the case of celiac patient; the celiac patient is characterized by an evident villi atrophy.*

In order to diagnose celiac disease, it is fundamental to evaluate villi atrophy by means of histological analyses, thanks to intestinal biopsy obtained during gastroscopy. Because of the high predominance of the celiac disease within the population (1%), it represents one of the main causes of malabsorption. Intestinal malabsorption diseases include also the intolerance towards carbohydrates, due to galactase deficiencies. In fact, galactase is one of the enzymes that are responsible of the scission of disaccharides into monosaccharides within the small intestine. The disaccharides which are not separated remain within the intestinal lumen, they hold liquids within

because of homeostasis, causing diarrhea and abdominal spread.

Another disease that provokes intestinal absorption deficiencies is white diarrhea (sprue tropicale). It is an acquired disease characterized by unknown etiology that is usually responsible for malabsorption, multiple nutritious deficiencies and alterations of small intestine mucosa. It is mainly common in Caribbean, in the south of India and in the south-east of Asia. The causes that are supposed to be responsible for the disease are bacterial, viral or parasitic infections, vitamins deficiencies and food toxins.

A rare disease, that is mainly common among men aging between 30 and 60 years old, is the Whipple's disease, provoked by the *Tropheryma whippelii* bacterium. The pathology is clinically characterized by anaemia, cutaneous pigmentation, articular symptoms, weight loss, diarrhea and heavy malabsorption. Small intestine mucosa is always damaged, as it is characterized by lesions observable during specific and diagnostic biopsies.

Intestinal lymphangiectasis is instead a syndrome characterized by a either congenital or acquired deformity of intramucous small intestine limphatic vessels. It affects mainly children and young adults.

Another pathology responsible for intestinal absorption deficiencies is the "short intestine" syndrome, which determines a typical inadequate absorption surface. It often results from either an extended intestinal resection or from jejenum-ileum bypass conceived as intervention against pathological obesity. An inadequate absorption surface causes consequently insufficient calories absorption and malabsorption of B12 and other vitamines, that can be responsible for acute poor nutrition with neurological deficiencies.

This general outline describing both the causes, the consequences and the physiological implications of intestinal malabsorption, allows to understand the importance of a physio-pathological *in vitro* model conceived as a useful tool to study the pathologies in terms of their dynamic development and characteristic features. This tool could allow also to develop and

optimize pharmacological focused effects

## 1.2 STATE-OF-THE-ART RELATIVE TO INTESTINE MODELS:

The model proposed is conceived as an *in vitro* tool, aimed at simulating the intestinal barrier, in terms of biological interface and of porous exchange and absorption path of drugs and solutes. The intestinal epithelium acts as a selectively permeable barrier, through the formation of complex protein-protein networks that mechanically link adjacent cells and seal the intercellular space. The protein networks connecting epithelial cells form three adhesive complexes: desmosomes, adherens junctions, and tight junctions. These complexes consist of transmembrane proteins that interact extracellularly with adjacent cells and intracellularly with adaptor proteins that link to the cytoskeleton **[46].** The predominant cell type in all absorbing regions is referred to as an enterocyte. Enterocytes are columnar epithelial cells that are bound to their neighboring cells at the luminal surface by tight junctions. Their apical cell membranes posses numerous microvilli which greatly increase the surface area available for absorption **[47].** At various portions of the absorbing regions, absorption is favored by mucosal structures such as fenestrations (small holes) in the endothelial cells of the capillaries, or pores of different sizes in the membranes of the enterocytes. Underlying the lamina propria is a thin layer of smooth muscle, the muscolaris mucosae. In regions of active absorption such as the small intestine, the muscular layer appears to be related to the rhythmic movements of the villi that agitate the layer of intestinal secretions and chyme that are in contact with the epithelium and thus promote absorption. The co-ordinated, rhythmic contractions of these layers of smooth muscle cause the intestinal motility which is responsible for the thorough mixing of chyme, the continual rejuxtaposition of chyme with the brush border of the enterocytes, and the propulsion of food through the GI tract in a net aboral direction (peristalsis). The majority of the absorbing surface area is found in the jejenum. In particular the small intestine is characterized by an absolute surface area of about 111 m2 and the large intestine of about 0.19 m2. The value relative to the absorbing surface area affects directly the absorption rate of substances. Chyme

traverses the human small intestine at a rate of 1–4 cm per min. The velocity of transport is faster in the proximal portions of the small intestine (duodenum and proximal jejunum) and decreases as chyme approaches the ileum. On average, chyme traverses the entire small intestine in 3–4 h. Transit time for chyme in the human large intestine is considerably slower. This paragraph represents a review of the approaches documented in the state-of-the-art on this topic. The commonly accepted intestinal absorption model consists of a layer of Caco-2 cells (cells of the human colon), cultured on a polycarbonate membrane within a transwell **[1,2, 10].** In this system, the compounds to be tested are added in correspondance to the apical side of the monolayer and the substances that pass through the cells are monitored in correspondance to the basolateral side. The traditional model poses some limitations, because the *in vitro* experiments are not able to reproduce many aspects of the *in vivo* behaviour. Cell cultures are characterized by substantial differences in comparison to the *in vivo* intestines phenotype, in terms of protein expression and cellular morphology. The limitation of the static monoculture is also related both to the use of a single cell type and to the lack of peristalsis, that reduces the overall permeability in comparison to the one measurable *in vivo.* The static condition represents a simplified model of the described physiological processes, which instead happen in a dynamic environment. The models proposed in the state-of-the-art, conceived as possible alternatives to the traditional one, belong to three main research fields **[18]:**

**SYNTHETIC-BIOLOGICAL MICROFABRICATED INTESTINE MODELS:**

The biomimetic models proposed tend to reproduce the *in vivo* microenvironment and they provide realistic *in vitro* models of intestinal villi, which are important to study and predict intestinal absorption.

A first example is the model proposed by Wang et al. **[19].** In this case, micromachining approaches were used to create a crypt-like microarchitecture, reproducing intestinal mucosa topography composed of crypts and villi onto polymeric substrates. Figure 1.13 depicts such structure.

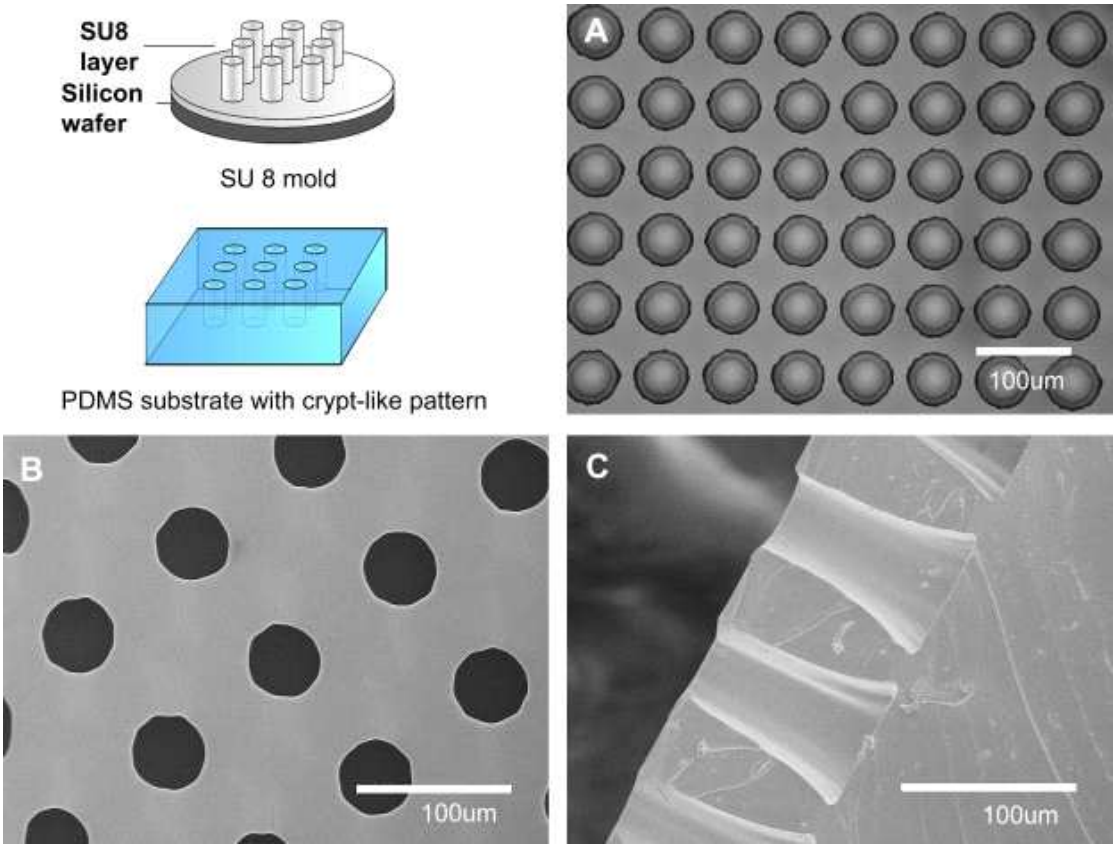


*Figure 1.13: Crypt-like structure microfabricated onto polymeric substrates: images of the structured mold, top view and section of the developed PDMS scaffolds.*

The superficial crypt-like topography guarantees a higher metabolic activity in comparison with a flat structure. This analysis was later reexamined, by adding a collagene type I membrane, properly designed and structured to study the synergy of the crypt-like structure and of the ECM proteins in terms of adhesion, proliferation and differentiation of intestinal Caco-2 cells and development of cell junctions **[20].** The importance of the crypt-like structure was evaluated in terms of short-term effects on the cellular phenotype, regarding Caco-2 cellular differentiation and enzymatic activity. On the other hand, the substrate surface chemistry, related to the ECM proteins used for the coating, affects the long-run behaviour of intestinal epithelial cells.

Gunawan et al **[21]** proposed a model in which they created protein gradients (laminin and collagen type I) similar to those found in the small intestinal crypts on an artificial substrate, by using microfluidic gradient generators. This study aimed at understanding the role of ECM proteins on the

intestinal epithelial renewal along the crypt-villus axis. Figure 1.14 depicts the model proposed.

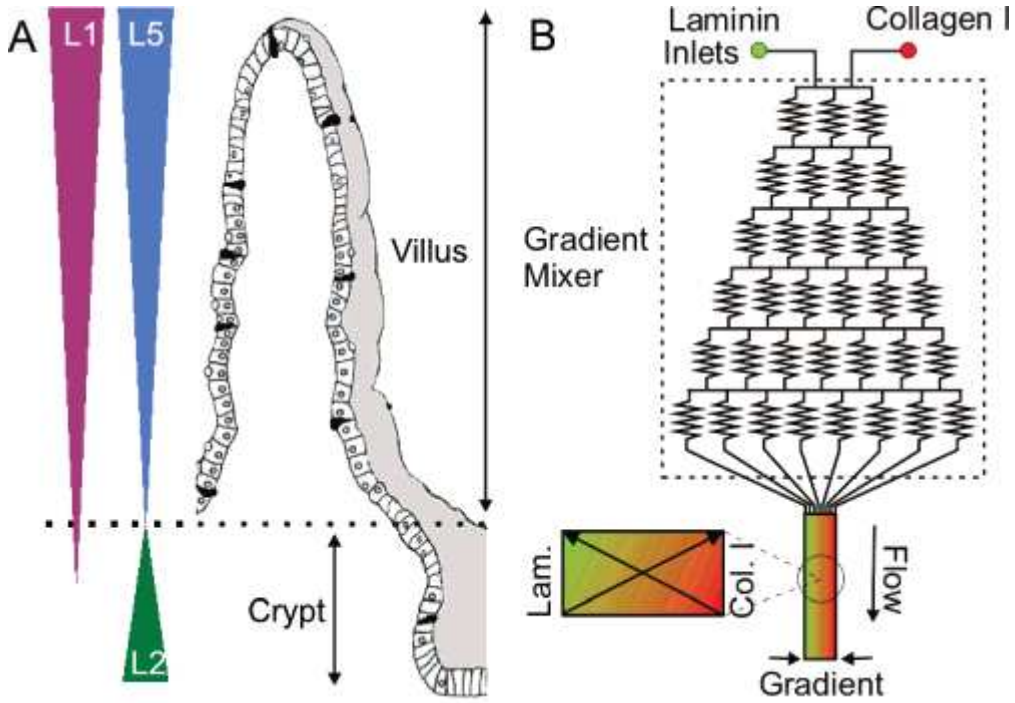


*Figure 1.14: ECM proteins pattern of crypt-villus epithelium obtained by using microfluidic platforms.*

Another emerging approach to engineer biomimetic GI tract is based on the use of hydrogels. Hydrogels have attracted great attention for 3D cell cultures since they mimic the ECM and can be easily modified to generate tailored microenvironments **[22-26].** Recently, Sung et al. developed a biomimetic GI tract model by using laser ablation combined with sacrificial molding in microscale collagen hydrogels mimicking the actual density and the size of the human intestinal villi **([27)].** Caco-2 cells seeded onto the structure covered the whole structure resembling finger-like intestinal villi covered with epithelial cells, figure 1.15.

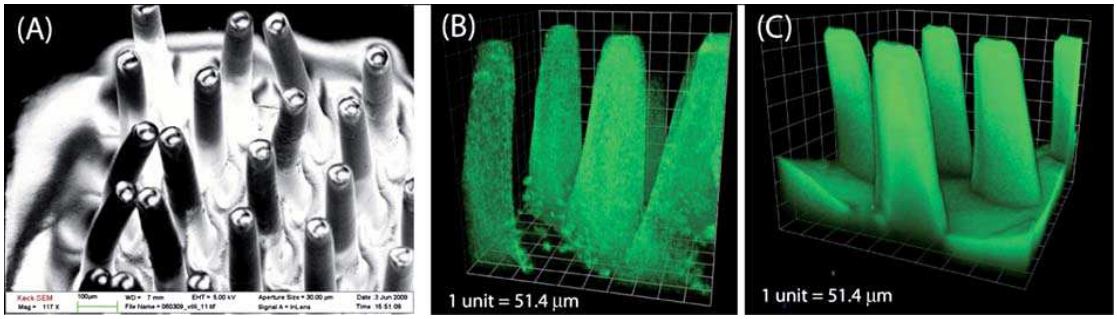


*Figure 1.15: SEM and fluorescence images of the structure composed of PDMS villi.*

In the paper **[28]** Shuler and his research group succeded in recreating the intestinal mucosa layer by the use of cellular lines representing intestinal epithelium, cells secreting mucine and lymphoid cells. The team realized a collagen structure representing the villi that cover intestinal epithelium and that allow absorption of drugs and substances. Finally another interesting work **([29])** was based on the fabrication of polymeric microporous membranes, either flat or containing controllable 3-dimensional shapes. Caco-2 cells were cultured onto the membranes to mimic key aspects of the intestinal epithelium such as intestinal villi and tight junctions (Figure 1.16). The developed membranes could be integrated with microfluidic, multi-organ cell culture systems, thus providing access to both sides, apical and basolateral, of the 3D epithelial cell culture.

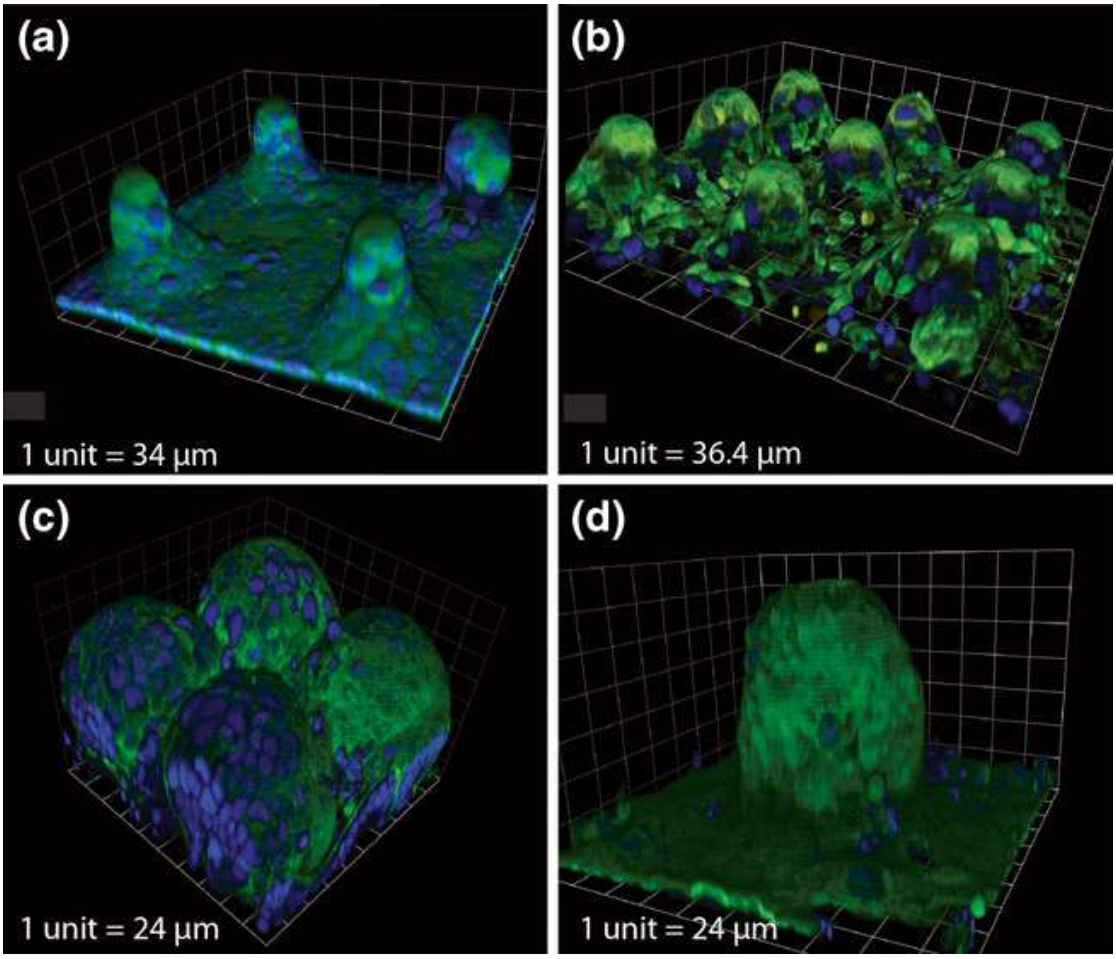


*Figure 1.16 :Images representing Caco-2 cell cultures on membranes characterized by silicon pillars.*

The papers proposed are characterized by the advantage of reproducing the morphological features of the *in vivo* environment (in particular the crypt-villus topography of the intestinal barrier), by the use of microfabrication techniques. They are models close to the physiological environment from the morphological point of view, but on the other hand this approach does not include the dynamic conditions that characterize the *in vivo* environment, such as fluid flow and peristalsis. These models are thus lacking of important factors that affect considerably the transit of substances through the intestinal barrier.

## 2. MICROFLUIDIC-BASED APPROACHES:

The field of microfluidics is increasing its relevance for drug discovery, development and personalized biomolecular diagnostics. Due to the ability of microfluidic systems to provide fluid

flow in physiological ranges, it offers spatial and temporal fluidic control in a biomimetic environment enabling long-term cell culture and spatial differentiation. Thus, microfluidics is becoming an integral part of cell-based assays to predict oral drug absorption. For realistic prediction of oral drug bioavailability, an *in vitro* model should incorporate all the major physiological obstacles to the drugs entry into systemic circulation. These include the transport properties of the epithelium, liver metabolism, and the vascular transport that links them. At this proposal, to overcome the limitations of monoculture systems, transwell co-colture models have been designed to include apical Caco-2 monolayers along with hepatocytes in the basolateral compartment **[30,31].** However, these models use large liquid to cells ratios and are devoid of circulatium of medium. To overcome these limitations, some solutions were proposed. To generate a biomimetic microenvironment for drug absorption studies, perfused co-culture systems based on microfluidics were designed. In the paper **[32]** Mahler et al for example co-cultured mucous secreting HT29-MTX goblet-like cells with Caco-2 cells to mimic intestinal cell populations and HepG2/C3A cell line as liver cell populations. Microfluidics has been also used to design a bioreactor system that allows to tune physiologically meaningful flow conditions in order to study various epithelial cell transport processes **[33,34,35].** Ferrel et al **[45]** fabricated a bilayer microfluidic system with integrated transepithelial electrical resistance (TEER) measurement electrodes to evaluate kidney epithelial cells under physiologically relevant fluid flow conditions. The apical and basolateral fluidic chambers were connected via a transparent microporous membrane. The top chamber contained microfluidic channels to perfuse the apical surface of the cells whereas the bottom chamber acted as a reservoir for transport across cell layer and provided support for the membrane. TEER electrodes were integrated into the device, to monitor cell growth and evaluate cell-cell tight junctions integrity in real time. Such bioreactors can be easily integrated with perfused co-culture systems that closely mimic GI epithelial barriers along with first pass metabolism described above. Kimura et al. developed a microfluidic device embedded within a stirred-based micropump, to create on-chip perfusion, and an optical fiber connection for on-line fluorescence

detection for drug screening and toxicity tests (**[36]).** In another study **[37],** a microfluidic device containing microhole arrays was fabricated, as an example of a microfluidic system used to study intestinal absorption. The device is a microchip-based system that mimics the intestine. The microchip was composed of a glass slide, a permeable membrane, and polydimethylsiloxane (PDMS) sheets, which contained microchannels made by photolithography; Caco-2 cells were cultured on the membrane in the microchip. The system was regulated with a microsyringe pump, that was able to generate slow pulsatile fluid flux. In particular, PDMS microchips are composed of two layers; each of them is endowed with microfabricated channels (apical and basolateral side) and with channels connecting the upper and the lower parts. The interface between the upper and the lower chambers is a BioCoat membrane, working as a scaffold that allows Caco-2 cells culture and growth. The microchip has two microchannels separated by a Caco-2 cells monolayer cultured on a porous membrane. These devices were used to perform permeability tests. The passage of two different substances characterized by a different ability to permeate through the intestinal barrier was assessed. The mixture containing the compound to be tested was added on the apical side, whereas the basolateral side contained the control fluid, representing the baseline.The final purpose of the work was to perform transport and absorption studies of substances and drugs through the intestinal barrier. This could be a useful tool for drugs screening in order to estimate their bioactivity. These models are able to mimic the dynamic conditions of the physiological environment and include cellular co-cultures that allow to overcome the limitations of the traditional monoculture model. On the other hand, these models are not able to mimic intestinal peristalsis, which is an important factor promoting the processes of transport of nutritious substances and drugs through the intestinal barrier.

## 3 MICROSCALE CELL CULTURE ANALOGS (µCCA):

This approach considers that drug absorption, distribution, metabolism and excretion is a result of the interactions between various cells, tissues and organs that are interconnected by vasculature.

In the state-of-the-art there are many physiologically-based pharmacokinetic models (PBPK), which describe an organism as a set of interconnected tissue or organ compartments based on vasculature. Their main purpose is to calculate the time-dependent distribution of a drug in various tissues **[38].** An important advancement in the field of drug screening is the integration of multiple miniaturized organ model systems into a single device to recapitulate the potential interaction between different organs. The concept of "microscale cell culture analogs" is a physical representation of PBPK model where different cell types are cultured in small chambers interconnected by fluidic channels **[39].** Such systems offer versatile *in vitro* models to study drug's biotransformation, and interaction between different tissues in determining drug's response (both efficacy and toxicity). The paper **[40]** is an interesting review that supplies an overview of the various approaches, provided in the state-of-the-art aimed at evaluating intestinal permeability and predicting pharmaceutical properties of biocompounds. An initial approach is based on the realization of *in vitro* models; their advantage is that they give the possibility to quantify the transport of substances through a cellular barrier. The main limitation of these methods is that they do not allow to quantify the amount of active drug transport observable *in vivo.* The review describes various methods proposed as alternatives to *in vitro* physio-pathological models. In particular, screening methods of membranes permeability are documented in literature as valuable alternatives to cell cultures. An example is the artificial phospholipidic membrane (paper **[41]**), obtained by soaking with phospholipids and with an organic solvent 96-well microtiter filter plates. The system allows to study the passive transmembrane transport, that is the main route of transport of drugs and other substances through the intestinal barrier. Recently, chromatographic methods aimed at modeling drugs intestinal permeability, have been studied. They allow to evaluate drugs interactions and/or their distribution in the membrane lipids, rather than quantifying the transport through them. In the state-of-the-art, some theoretical models of the intestinal permeability were introduced; they represent valuable alternatives to the wide spectrum of *in vitro* and *in silico* models. Theoretical models allow to estimate intestinal permeability and they are based on the

most meaningful parameters that describe the subject matter of the research. In particular, the models contemplate the calculation of lipophilicity, hydrogen bonding and molecular dimensions **[42,43].** These computational approaches, aimed at predicting the transport through the membrane, allow the prediction of passive transcellular transport and subsequently the development of a theoretical reference model. The ability of a molecule to permeate a cell depends on the number and the strength of the hydrogen bonds that the molecule forms with water. Drug lipophilicity instead is a predictor of membrane permeability, since it is assumed that drug partitioning into the (lipophilic) cell membranes is a rate-determining process for passive membrane permeation. The process of partitioning within the membrane is a two-step process led by two decisive forces for the permeability rate through the membrane: lipophilicity and hydrogen bonds forming potentiality. The theoretical models take into accout other predictors of passive transport through the membrane, such as: solute size, molecular surface properties (they depend on drug molecules shape and on their steric hindrance) and Polar Surface Area (PSA). PSA is defined as that part of molecular surface area contributed by nitrogen and oxygen atoms, plus the area of the hydrogen atoms attached to their heteroatoms. Many studies demonstrate the correlation between "non polar surface area" and intestinal permeability. Approaches based on quantum mechanics calculations have recently been used to predict passive membrane permeability to drugs and other compounds. Norinder et al. developed a method for predicting Caco-2 cell monolayer permeability to a series of structurally diverse conventional drugs. They used molecular mechanics methods and the global minimum conformation, that was then subjected to a further semi-empirical structural optimization. These approaches,that were quoted to obtain a complete overview, take into account physical properties and electronic effects (for example charge distribution) to build up theoretical prognostic models of membrane permeability based on proper parameters.

## 1.3 OVERVIEW OF LOCs (Lab On Chip Technologies) AND CURRENT DRUG TESTING SYSTEMS:

LOC (Lab On Chip) technologies aim at developing biomimetic *in vitro* models. These models tend to reproduce the main functional properties of various organs and tissues and consequently to simulate various physiological and pathological conditions. The purpose is to preliminarly study physiological phenomena and to predict the *in vivo* behaviour and metabolism. Cell chips allow elegant and systematic design of various physiological factors such as extracellular matrix, cell-to-cell communications, molecular concentration gradients. In the state of the art various organ-mimetic microdevices with integrated functionalities were proposed. They reproduce key structural, functional, biochemical and mechanical features of living organs. They offer a tool *in vitro* aimed at simulating important processes characteristic of particular diseases and strictly dependent on 3D organ architecture. Other systems that envisage 3D cell cultures have been also developed. They overcome the limitations of bidimensional models and they try to compensate their deficiencies in reproducing the microenvironment *in vivo.* "Organs on chip" integrate microfluidic technologies and living cells cultured in 3D microfabricated devices, to study human phisiology in a context organ-specific, to develop *in vitro* models of specific pathologies and to create 3D models able to replicate more complex structures at organ or biological interface level.

Miniaturized cell chips **[3]** are characterized by the following main advantages in respect to the limitations characterizing the traditional tools:

- reduction of cell/drug consumption (important for rare cell analysis and cost reduction) ;
- high surface area-to-volume (SAV) ratio, that facilitates heat transfer to achieve precise temperature control for healthy cell culture;
- laminar fluid flow and diffusion-dominated mass transport process, to well resemble the *in*

*vivo* condition;

- Integration of different functional units for cell-drug reaction, cell sorting and cell response detection to allow serial processing and analysis of various cell/drug samples;
- massive parallelization of miniaturized functional units to achieve high throughput and multi-parametric analysis of drug induced cellular responses;
- more accurate control of the cellular microenvironment and a decrease of the biological variability between different cells and cultures;
- major predictive potentiality of the response and consequently economic advantages in drug testing experiments;
- possibility to manage with miniaturized devices that are characterized by low manufacturing cost.

In general, on-chip technologies include two categories:

- MICROFLUIDIC CELL CHIPS: they are tipically composed of microchannels with several functional units such as micropumps and microvalves to transport drug compounds to target cells.
- NON-FLUIDIC CELL CHIPS: they usually consist of solid supports where small volumes of cells can be displayed in defined locations, allowing multiplexed interrogation and analysis of living cells (microwell cell chips, micropatterned cell arrays etc).

As most part of drugs screening methods involve the cellular expression of recombinant targets and subsequently the study of cell-drug interactions by rapid and quantifiable assays, the merits of a cell chip make it an ideal tool to investigate cell-drug interactions. Since the model proposed in this work envisages a possible future application in drug testing systems, subsequently an overview about the main systems developed so far is proposed in order to contextualize the matter. Recently

novel microfabrication technologies were developed; they allow to interface the cells with drug testing systems. They are integrated systems that include cell cultures and engineered tools designed *ad hoc* for the specific application. The paper **[14]** aimed at engineering cellular microenvironments to improve cell-based drug testing and systemic toxicity studies.

Another example of this type of systems is the paper **[15].** It proposes a drug-screening *in vitro* platform for drug screening based on the contractility of tissue-engineered muscle. A tissue-based approach to *in vitro* drug screening allows for determination of the cumulative positive and negative effects of a drug at the tissue rather than the cellular or subcellular level. Skeletal muscle myoblasts were tissue-engineered in three-dimensional muscle with parallel myofibers generating directed forces. The miniature bioartificial muscles were able to generate tetanic (active) forces upon electrical stimulation measured with a novel image-based motion detection system. The tool proposed is a system that allows to evaluate tissue or organ-specific effects caused by different compounds. The results described in the paper demonstrate the integration of tissue engineering and biomechanical testing into a single platform for the screening of compounds affecting muscle strength. In particular the authors analyzed the muscle response to compounds that increase or decrease muscolar hypertrophia and contractile strength. The muscolar force in response to different types of drugs was measured. In particular, changes of muscolar contraction are symptomatic and representative of the general effects induced by a compound at the expense of all of the biochemical mechanisms that are involved in the process of force generation.

Some other meaningful studies belonging to this research domain are described below. Ingber et al. designed and realized a lung-on-chip device (**[4]**). This biomimetic microsystem reconstitutes the critical functional alveolar-capillary interface of the human lung. This bioinspired microdevice reproduces key functional, structural and mechanical properties of the alveolar-capillary interface, that is the fundamental unit of the living lung. This was accomplished by microfabricating a microfluidic system containing two closely apposed microchannels separated by a thin (10 μm),

porous, flexible membrane made of poly (dimethylsiloxane) PDMS. The intervening membrane was coated with ECM (fibronectin or collagen), and human alveolar epithelial cells and human pulmonary microvascular endothelial cells were cultured on opposite sides of the membrane. Once the cells were grown to confluence, air was introduced into the epithelial compartment to create an air-liquid interface and more precisely mimic the lining of the alveolar air space. The system involves two lateral microchambers. When vacuum is applied to these chambers, it produces elastic deformation of the thin wall that separates the cell-containing microchannels from the side channels; this causes stretching of the attached PDMS membrane and the adherent tissue layers. This design replicates dynamic mechanical distortion of the alveolar-capillary interface caused by breathing movements: that is the mechanical forces acting on the cells when the individual's thorax expands and contracts. Figure 1.17 depicts the structure of the described model.

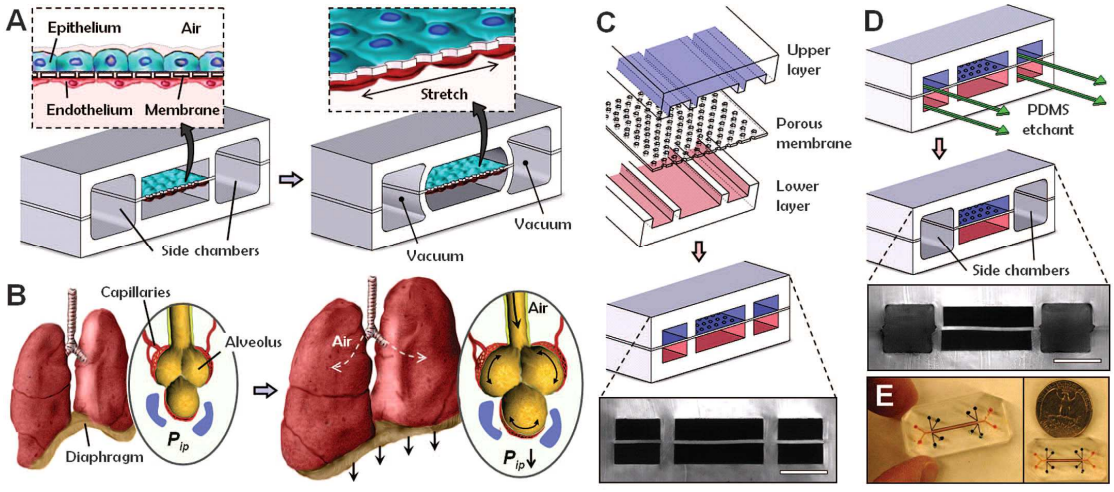


*Figure 1.17: Structure of the lung-on-chip bioinspired microdevice.*

The study demonstrated that epithelial cells were able to reproduce the permeability of the barrier within the microsystem and that their behaviour changed when they are stretched. The system was conceived for direct and quantitative evaluation of various biological processes of the human lung and it overcame the limitations of both animal and of traditional cell cultures models. The device allowed the application of cyclic stretching and fluid shear stress to two opposing cells layers

separated by a permeable and flexible ECM, while simultaneously enabling analysis of tissue barrier permeability and transport. The microsystem on-chip proposed in the paper was also validated in the case of the simulation of more complex integrated organ-level responses, observed in whole living lung, such as pulmonary inflammation, by incorporating blood-borne immune cells in the fluid flowing through the vascular channel. The bioinspired microdevice was evaluated also for nanotoxicology studies, thanks to the pulmonar response to nanoparticles released in correspondence of the epithelial compartment. The authors demonstrated that cyclic mechanical strain accentuates toxic and inflammatory responses of the lung to silica nanoparticles. The importance of the model proposed consists of the combination of a biohybrid tool simulating a tissue-tissue interface and of an actuation system replicating the breathing movements of the organ. The final purpose is obtaining a biomimetic device as more plausible as possible, in respect to the *in vivo* behaviour. The proof-of-concept of this research work is similar to the model proposed in Ingber's paper. The basic idea is infact engineering an interface between epithelial and muscolar tissues, in order to reproduce the intestinal barrier in terms of both permeability and peristalsis. The model proposed infact can be actuated in order to reproduce the peristaltic movements of intestines *in vivo.* Peristalsis infact represents a key feature both in terms of metabolic and of transport processes.

Another example of "organ-on-chip" is the system "artery-on-chip" (**[5]**). It consists of a device designed to study "resistance arteries". They are blood vessels characterized by small diameters, that contribute to the regulation of the blood flow lead into the capillaries lumen, to prevent their damage. The blood vessel was at first removed from a mouse and it was then sutured at the extremities. Both inside and outside the vessel the *in vivo* physiological pressure was replicated. The device allows the researchers to insert a blood vessel within a microfluidic chip. A chamber designed *ad hoc* allows to maintain the blood vessel in a defined desired location, supplies liquid continuosly through it and allows to analyze a set of drug doses and different timing, by the use of a computer controlled system.

Another important system documented in literature (**[7]**) is aimed at replicating bone structure by the use of an array of PDMS microchambers interconnected by narrow (1µm wide) channels. The device was similarly used to enable growth and *in vivo*-like reorganization of osteocytes in a structured 3D environment. Other examples include a compartmentalized microfluidic system **[6]** that enables co-culture of neurons and oligodendrocytes to study neuron-glia communication during development of central nervous system and a microdevice **[8]** incorporating ECM gels microinjected between two parallel microchannels to investigate the vascularization of liver tissues in 3D culture microenvironments. The paper **[9]** describes an example of tissue engineering as a promising approach for esophageal replacement, to reconstruct *in vitro* esophageal walls. The researchers analyzed the feasibility and the optimal conditions of human and pig skeletal myoblasts (HSM and PSM) and porcine oral epithelial cells (OEC) culture on biologic scaffolds. Myoblasts proved to be able to differentiate and to promote the renewal of damaged muscolar fibers. Epithelial cells accelerate the process of muscle renewal and prevent the stenosis subsequent to circumferential esophageal replacement. The paper highlights the importance of the use of co-cultures in tissue engineering; the approach proposed is hybrid and it combines matrixes and cellular co-cultures.

This research field involves also the development of *in vitro* physio-pathological models of particular diseases. An example is a device fabricated by the use of two layers of PDMS micro channels, stacked and separated by a thin porous membrane. The device is used to create eterothipic multicellular spheroids in a 3D microfluidic culture system, that reproduces the cancerous microenvironment of prostate metastatic cells **[44]**.

A further development of this research field is aimed at the development of multi-micro organoid chips. These chips are *in vitro* models that do not represent a single organ on its own, but they simulate the crosstalk and the interactions among various organs. This analysis is important in the context of systemic toxicity studies. This researc field is aimed at the development of models

composed of interconnected compartments, each one of them representing a distinct organ. The various constituent organs are interconnected by a microfluidic circulatory system. In the state-of-the-art, there are several interesting examples. Some of them are based on silicon wafers "etching", to obtain little compartments that could include intestinal, epathic and adipose tissue cells, interconnected by microfluidic channels. The paper **[11]** proposes another alternative solution for drug testing to predict human exposure, by the use of "human multi-micro-organ" systems composed of miniaturized bioreactors. The authors designed and simulated a system that envisages long-term dynamic on chip cultures of the smallest functional units of human organs, called "micro-organoids". Every chip contains six identical micro bioreactors. Each bioreactor contains three different micro-organoids culture segments, a nutritious substances supply and a reservoir. In particular micro-organoids segments of liver, cerebral cortex and bone marrox were cultured within each bioreactor. The platform of the device is dedicated to maintain human micro-organoids of liver, bone marrow and cerebral cortex within a systemic and controlled micro environment. The recent advance in range of Lab On Chip Technologies are "human-on-chip" systems, that represent an interesting future perspective. This research field concerns the development of 3D models aimed at simulating the metabolism and the physiology of the whole organism by the use of a system composed of compartments interconnected by a vascular network. In the paper **[12]** Esch et al. proposed an example of "human-on-chip" system. It consists of a microfabricated bioreactor containing 2D cultures of hepatic and pulmonary cells within distinct micro chambers, connected by microfluidic channels. The system was later modified with the addition of either 2D or 3D cultures of fat cells, cancer cells and marrow stem cells. It is aimed to appreciate systemic drug accumulation, distribution and absorption.

## 1.4 MODEL PROPOSED:

The device proposed in this Thesis is a biomimetic tool aimed at simulating the intestinal barrier, both as an interface that allows substances transport and drug absorption and as an engineered biohybrid actuator that reproduces intestinal peristalsis. The intestinal peristalsis is in fact an important factor that promotes the transit of bio-compounds in the GI tract and the transport and absorption of drugs and solutes through the intestinal barrier. The model mimics the intestinal barrier as permeable selective interface by the use of an engineered porous PLA nano-membrane. On the opposite sides of the membranes Caco-2, cells of intestinal epithelium and contractile cardiac muscle cells were cultured. Muscle stretch the supporting membrane and subsequently actuate the overall device, thanks to their capacity to develop active contractile force. Theoretically it should be necessary to use smooth muscle cells, to obtain a more plausible model of the anatomical structure of intestinal barrier *in vivo.* However, their contraction has to be induced by external electrical stimuli, so in this case it would be indispensible to integrate bioelectrodes in the system. The problem was splitted in multiple levels of difficulty, because the initial purpose was really ambitious. In this initial prototype the problems due to external electrical stimuli to contract the muscolar fibers and due to the integration of bioelectrodes in the system were neglected and removed. Smooth muscle cells were thus replaced with cardiomyocites, characterized by spontaneous contraction and not needing external stimuli.

# 2. MATERIALS AND METHODS

## 2.1 DEVELOPMENT OF POROUS NANOFILMS

In the firts phase of the Thesis, different fabrication techniques aimed at developing porous nanofilms were evaluated. The first attempt was based on spin coating deposition of a dispersant poly (lactic-co-glycolic)acid (PLGA polymeric solution) containing a disperse phase of a porogen (water-soluble) particulate. Salt leaching was then performed in deionized water. The second approach relied on a fabrication technique, based on soft lithography. This last procedure aimed at developing a micro-patterned mold to be exploited for achieving a porous nanofilm with a highly controllable structure.

### 2.1.1 Microfabrication technique based on spin coating and salt leaching

The salt leaching technique is one of the most common microfabrication methods used to develop porous scaffolds. The procedure is based on a mixture of a dispersant solution, insoluble in water, containing particles of a water-soluble porogen in suspension. When the mixture is immersed in water, the porogen is dissolved and subsequently determines the presence of pores in the resulting scaffold. The microfabrication technique investigated in this Thesis is based on spin coating deposition of a PLGA thin polymeric film containing water-soluble porogen particles and further salt leaching in deionized water. The analysis included the comparison between two different porogens, namely glucose and sodium chloride, a set of concentrations of the PLGA polymeric solution and different spinning speeds.

**Poly (lactic-co-glycolic) acid (PLGA)**

PLGA is a copolymer which is widely used to develop therapeutic devices, thanks to its

biodegradability and biocompatibility. PLGA is synthesized by means of random ring-opening co-polymerization of two different monomers, glycolic acid and lactic acid. It is characterized by the molecular formula shown in Figure 2.1:

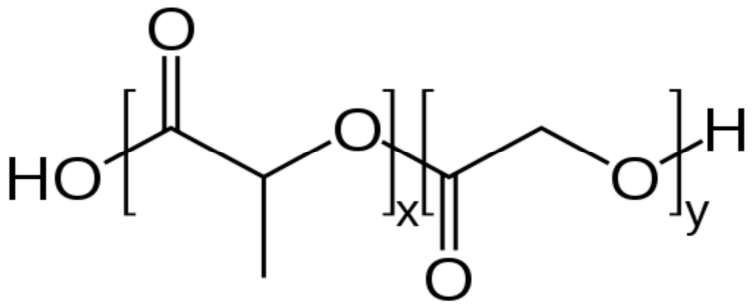


*Figure 2.1: PLGA molecular formula.*

PLGA degrades by hydrolysis of its ester linkages in the presence of water. The time required for degradation of PLGA is related to the monomers'ratio used in production: the higher the content of glycolide units, the lower the time required for degradation. PLGA has been successful as a biodegradable polymer because it undergoes hydrolysis in the body to produce the original monomers, lactic acid and glycolic acid. These two monomers, under normal physiological conditions, are by-products of various metabolic pathways in the body. Since the body effectively deals with the two monomers, there is minimal systemic toxicity associated with using PLGA for drug delivery or biomaterial applications. Even if PLGA is a biodegradable polymer, the time duration required for its degradation is rather long and it results thus negligible for our purposes. PLGA characteristics which guarantee its massive use are both its high biocompatibility and the possibility to use the polymer efficiently in order to obtain thin films.

**Polyvinyl Alcohol (PVA):**

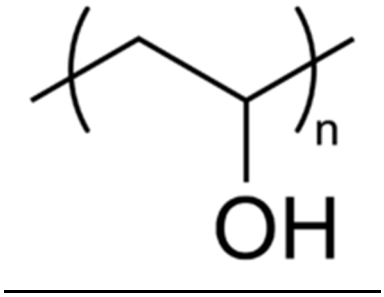


*Figure 2.2: PVA molecular formula.*

PVA is a water-soluble synthetic polymer, which is odourless, colorless and insoluble in organic solvents. Thanks to these properties PVA can be used as an efficient water-soluble sacrificial layer. PVA has an excellent capability to form films. In this Thesis, PVA was used to develop water-soluble sacrificial layers.

**Spin Coating**

Spin coating is a common micro/nano fabrication procedure used to deposit uniform thin films onto flat substrates. Usually a small amount of coating material is applied on the center of the substrate. The substrate is then rotated at high speed in order to spread the coating material by centifugal force. The film final thickness is the result of the combination of two determining parameters: spin coating procedure duration and spin speed. Higher spin speeds and longer time duration allow to attain thinner substrates. After high-speed spin coating, the sample is heat-treated; this phase allows to dry the sample, without further reducing its thickness. This step is fundamental to guarantee the physical stability of the sample and to consequently avoid further problems of film handling. Acceleration is another crucial parameter. In fact, in many processes, half of the solvent

tends to completely evaporate during the initial seconds. Furthermore, acceleration affects also coating properties of patterned substrates. In fact, while the spinning process is responsible for the radial outwards force, the acceleration determines on the material a twisting rotational force. The twisting force contributes to the dispersion of the material on the entire surface of the substrate **[54].** The spin coater used is WS-650 spin processor model, Laurell Technologies Corp., North Wales, PA. All the routines for PLA nanosheets fabrication were conducted in a clean-room (class 1000) to avoid contamination.

**Experimental procedure**

**Porogen preparation and characterization**

The porogens (glucose and sodium chloride, both puchased from Sigma Aldrich) were at firts grinded in a ceramic mortar and later sifted, in order to control the maximum size of porogen grains. The analysis included different time durations of the pounding phase: 5, 10, 15 and 20 minutes, respectively. The sifting phase instead consisted of two serial steps, based on the use of sieves having knit size of 63 μm and 38 μm. The choice allowed to control the porogen grain dimensions and to set a maximum admissible size. Grain dimensions were quantified by means of SEM analysis of the porogen particles, previously dissolved in dichloromethane and, after the complete evaporation of the solvent, gold sputtered and imaged.

**Fabrication of porous PLGA nanofilms by means of spin coating and salt leaching**

Silicon wafers (Si-Mat Silicon Materials, Kaufering, Germany) were used as substrates for the spinning technique. The silicon wafers were cut in 2*2 cm pieces, then cleaned with acetone and

isopropyl alcohol, throughly rinsed by deionised water, to ensure acetone removal and finally dried by an air flux.

A solution of PLGA in chloroform was mixed with the two porogens (glucose and sodium chloride). Two different PLGA concentrations and a set of porogen fractions, suspended within the PLGA solution, were tested and compared. Table 2.1 resumes the cases analyzed**:**

| **PLGA concentrations [mg/ml]** | **Glucose concentrations [mg/ml]** | **Sodium chloride concentrations [mg/ml]** |
|---|---|---|
| 100 | 100 | 5 |
| 50 | 10 | 1 |
| | 5 | 0,5 |
| | 1 | |

*Table 2.1***:** *Schematization of the different concentrations of both the dispersant and the two disperse phases analyzed.*

A PVA ($M_w$ 13000-23000, 98% hydrolyzed) aqueous solution (1% w/ v) was deposed by spin-coating on a silicon wafer (at 4000 rpm for 20 s) forming the water-soluble sacrificial layer, promoting film detachment from the wafer itself.

Then the emulsion, composed of PLGA and porogen, was spin-coated on the first layer, by maintaining the same spinning parameters (3000 rpm, 20 s) in all the cases. After drying the samples (at 80 °C for 1 min), they were immersed in deionized water in order to dissolve both the sacrificial layer and the porogen particles. As a consequence, the PLGA nanofilm was released free-standing in liquid and the porogen was leached out in water. The resulting nanofilms were finally analyzed by SEM imaging.

## 2.1.2 MICROFABRICATION TECHNIQUE BASED ON PHOTOLITHOGRAPHY

**Development of patterned molds**

Lithography refers to a family of micro/nano fabrication techniques used to pattern parts of a thin film or the bulk of a substrate, useful to develop or to replicate microstructures. These techniques allow to develop patterned molds having a well-defined topography, by the use of a photomask designed *ad hoc* as a function of the desired prototype. The photomask consists of a glass substrate with a thin chrome layer on its surface, characterized by a precise pattern. Chrome is not transparent to UV light; this property guarantees the possibility to expose to UV light precise areas through the mask, not covered by the opaque chrome layer **[55].** Photolithography uses light to transfer a geometric pattern from a photomask to a light-sensitive chemical "photoresist", on the substrate. The photoresist that are sensitive towards UV light can be either positive or negative, according to the reaction activated by the interaction between the UV rays and the material. Positive photoresists, after UV exposure, start to reticulate, whereas negative photoresists do not reticulate during post-bake phase subsequent to UV exposure. In particular, positive photoresists after UV exposure become more soluble in the developer solution, allowing the removal of the exposed areas. UV exposure infact modifies the chemical structure and the properties of the material, and particularly its solubility in the developer solution. The post exposure rinsing in the developer solution allows to replicate on the wafer a pattern mold, that is the exact replica of the photomask. Negative photoresists behave in an opposite way. In this case in fact, after UV exposure, the resist polymerizes and becomes consequently less soluble in the developer solution. The negative resist, after UV exposure is not removed by the developer solution, but remains on the surface. In this case the areas that are removed are in fact those not directly exposed to UV light. In the case of negative photoresists, the photomask is characterized by the inverse pattern in respect to the structure that has to be impressed on the silicon substrate **[56].**

- A photomask was designed *ad hoc* by means of Autocad, in order to obtain patterned molds

characterized by a well-defined topography. The photomask was provided with cylindrical pillars having diameters of about 5 μm and mutual distances between adjacent pillars of 5 μm. This choice would allow to obtain as a final result nanofilms having theoretically an average porosity of about 20%.

- Silicon wafers were cleaned at first with acetone and isopropyl alcohol, thoroughly rinsed by deionised water and dried. The chemical treatment of the silicon wafers aimed at removing organic or inorganic contaminations that are present on the surface. Cleaned wafers were finally dehydrated by means of thermal treatment at 120 °C for 30 minutes, to drive off any moisture that may be present on the wafer surface.
- A MICROPOSIT PRIMER solution was deposed by spin-coating on a silicon wafer, by using constant spinning parameters [3500 rpm, 30 s], to promote adhesion of the photoresist to the wafer.
- A positive photoresist SHIPLEY S1813 was deposed by spin-coating on the first layer. The set of photoresist spin coating speeds that were tested is listed in Table 2.2**:**

| **Photoresist spinning speed [rpm]** |
|---|
| 1500 |
| 2000 |
| 2500 |
| 3000 |

*Table 2.2: photoresist spin coating speeds.*

The time duration of the photoresist spin-coating phase was instead maintained constant and in particular equal to 35 s.

- After photoresist spin coating deposition, the samples were baked at 120 °C for 1 min, to drive off excess photoresist solvent.
- The wafers, previously coated with S1813 positive photoresist, were later exposed for 0.5 s to UV light by the use of a Mask Aligner in hard contact operating mode. UV exposure allows to imprint on the silicon wafer the desired pattern, causing a chemical change that allows some of the photoresist to be removed by the developer solution.

- The samples were immersed in AZ DEVELOPER solution for 1 s to selectively dissolve the exposed photoresist areas.
- The developed samples were later rinsed by deionized water and dried with compressed air.
- They were finally post-baked by means of a thermal treatment at 120 °C for 1 min.

**Development of porous nanofilms:**

Porous nanofilms were developed thanks to spin-coating deposition on patterned molds of a PLA polymeric film, on a firts layer of PVA water-soluble sacrificial layer.

**Polylactide acid (PLA):**

The compound used for nanofilm fabrication was PLA, purchased from Sigma-Aldrich (cod= 94829 Mw= 67000 Mn=50000). PLA is characterized by the molecular formula shown in Figure 2.3:

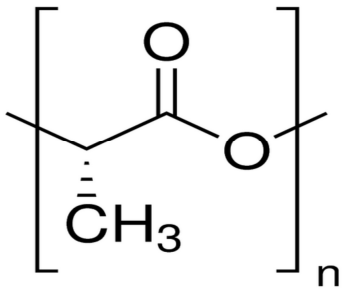


*Figure 2.3: PLA molecular formula.*

PLA, a lactic acid polymer, is a thermoplastic aliphatic polyester. Due to the chiral nature of lactid acid, two distinct enantiomeric forms of polylactide exist: L and D. PLLA is the product resulting from polymerization of L, L-lactide. PLLA has a cristallinity of around 37%, a glass transition temperature between 60-65°C, a melting temperature ranging between 173 °C and 178 °C and a tensile modulus between 2.7-16 GPa **[57].** PLA is able to degrade into lactic acid. Lactic acid is a compound at all innocuous in the biological environment. Lactic acid biocompatibility is a key factor that allowed us to select it for nanofilm fabrication, despite its degradability (anyhow, PLA

degradation rates are rather slow**:** it normally degrades in more than one year).

In this Thesis, PLA (2% w/v in dichloromethane) was used to fabricate porous micro-/nano- films characterized by controlled thickness and porosity.

**Dicholoromethane**

Dichloromethane (or methylene chloride, DCM) is an organic alkyl halide compound that is widely used as a solvent. Although it is not soluble in water, it is miscible with many organic solvents. The molecular structure of the compound is shown in Figure 2.4:

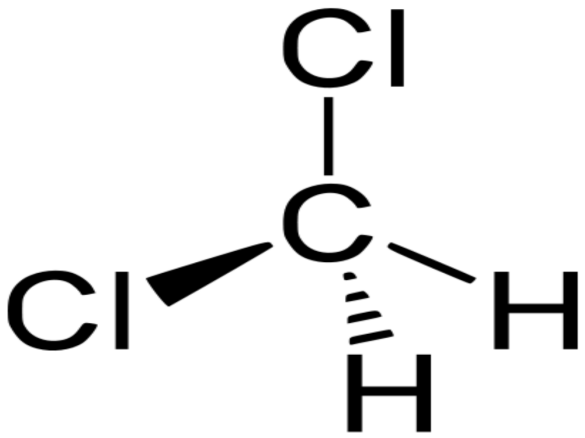


*Figure 2.4: Dichloromethane molecular formula.*

At room temperature dichloromethane is a colorless, volatile liquid with a moderately sweet aroma. DCM is considered noxious and potentially carcinogenic, even if less than other solvents such as chloroform. DCM's volatility and ability to dissolve a wide range of organic compounds makes it a useful solvent for many chemical processes.

**Fabrication of porous nanofilms by means of spin coating on patterned molds**

At first a PVA aqueous solution (1% w/v) was first deposed by spin-coating (4000 rpm, 20 s) on

a patterned mold, previously gold-sputtered (25 mA, 60 seconds) and plasma-treated . Thanks to the inert gold coating, gold sputtering prevented the PLA solution from chemically reacting with the underlying photoresist layer. Plasma treatment instead enhanced the hydrophile of the patterned mold and consequently increased the adhesion of PVA. The plasma treatment, achieved by using Colibrì plasma reactor purchased from Gambetti, was characterized by the following parameters**:**

- **Plasma Time:** 90 s
- **Power Set Point:** 30 W.
- **Gas stb time:** 0 s.
- **Oxygen setpoint :** 50%.

As mentioned, PVA formed the sacrificial layer. A following solution of poly (lactic acid) in dichloromethane (PLA 2% w/v ) was then spin-coated on the first layer by using the spinning parameters listed in Table 2.3**:**

| **PLA Spinning Parameters** |
|---|
| 3000 rpm, 20 s |
| 4000 rpm, 20 s |
| 5000 rpm, 20 s |
| 6000 rpm, 20 s |
| 7000 rpm, 20 s |

*Table 2.3***:** *PLA spin coating parameters*

After drying the sample (80 °C; 1 min), the PVA sacrificial layer was dissolved in water thus releasing the PLA nanofilm free-standing in liquid.

## 2.2 SAMPLE CHARACTERIZATION:

### 2.2.1 ATOMIC FORCE MICROSCOPE (AFM)

Atomic Force Microscope AFM is a very high-resolution type of scanning probe microscope (SPM), which demonstrated resolution on the order of fractions of a nanometer and allows to attain an image at the atomic level of the scanned surfaces. AFM consists of a cantilever with a sharp tip (probe) at its end that is used to scan the specimen surface. The two main components of AFM are the probe and the scanner. The tip, which scans the various areas of the sample, is the interface between SPM and the sample itself. The scanner, instead, controls with high precision the position of the probe in respect to the surface, both horizontally and laterally. As the tip is brought very close to the surface of the object under investigation, the *Van der Waals* forces acting between the tip and the sample lead to a deflection of the cantilever according to Hooke's law, which is the what the AFM is designed to measure. A spatial map of the interaction can be made by measuring the deflection at many points of a 2D surface. Cantilever deflection is measured using a laser spot reflected from the top surface of the cantilever into an array of photodiodes. Figure 2.5 shows this operating principle:

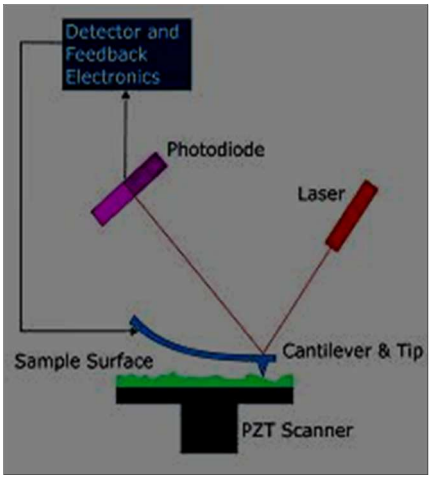


*Figure 2.5*: *AFM operating principle.*

The AFM can be operated in a number of modes, depending on the specific application. In general, the possible imaging modes can be divided into static and (also called *contact)* modes and a variety of dynamic (*non contact or tapping)* modes where the cantilever is vibrated. AFM operation is usually described as one of three modes, depending on the nature of the tip motion:

***Contact mode (STATIC MODE):*** the tip is 'dragged' across the surface of the sample and the contours of the surface are measured either using the deflection of the cantilever directly or, more commonly, using the feedback signal required to keep the cantilever at a constant position.

**Tapping mode*:*** In the tapping mode the cantilever is driven to oscillate up and down at near its resonance frequency by a small piezoelectric element mounted in the AFM tip holder similar to non-contact mode. The amplitude of the oscillation is modified by the interaction forces between the tip and the sample surface. Van der Waals forces, dipole-dipole interactions, electrostatic forces are responsible for the amplitude of this oscillation to decrease as the tip gets closer to the sample. An electronic servo controls the height of the cantilever above the sample by using the piezoelectric actuator. The servo adjusts the height, in order to maintain a set cantilever oscillation amplitude as the cantilever is scanned over the sample. A tapping AFM image is therefore produced by imaging the force of the intermittent contacts of the tip with the sample surface. The variations of the oscillation in relation to the external reference oscillation give information about the superficial features of the sample scanned.

***Non contact mode*** In this model the tip of the cantilever does not contact the sample surface. The cantilever is instead oscillated at either its resonant frequency (frequency modulation) or just above (amplitude modulation) where the amplitude of oscillation ranges typically from a few nanometers to a few picometers. The Van der Waals forces, which are the strongest from 1 nm to 10 nm above the surface, or any other long-range force that extends above the surface act to decrease the resonant frequency of the cantilever. This decrease in resonant frequency combined with the feedback loop system maintains a constant oscillation amplitude or frequency by adjusting the

average tip-to-sample distance. Measuring the tip-to-sample distance at each data points allows the scanning software to construct a topographic image of the sample surface.

The AFM used in this Thesis is Veeco Innova Scanning Probe Microscope. The samples, having dimensions of 1 cm*1cm, were at first positioned on a proper supporting metal small disc. The software used to control by computer the AFM probe and to set the proper scanning parameters is SPMLAB 7.20. By means of the 'Motor Stage' function provided by the software, the tip was raised, before positioning the sample on the proper location, in order to guarantee a sufficient tip-sample distance and to thus prevent from either breaking or damaging the tip itself. After the sample positioning in the proper location, by the use of the 'Motor Stage' SPMLAB 7.20 function, the tip was brought closer to the sample surface. Before starting sample scanning it is fundamental to guarantee both a proper detector alignement and a suitable cantilever resonant frequency.

The parameters used to set the cantilever resonant frequency were:

- **Range:** 0-1000KHz
- **Drive Amplitude:** 1 V
- **Input Gai:** x4
- **Target tapping signal:** 7 V

Finally, AFM tip was engaged to the sample surface and the following scanning control parameters were set:

- **Samples/ line:** either 256 or 512, in the case of high-resolution images.
- **Scan rate:** 0.3 Hz
- **Scan range:** 50.00 µm
- **Rotation:** 0

SPMLAB 7.20 software is furthermore endowed with a proper tool conceived for image analysis, which allows to analyze and elaborate the images of the scanned sample. Some of the functionalities offered by the image analysis tool are i.e. 'Leveling', which allows to choose the points of the image that lie on the same plane, '3D Display' which performs a tridimensional map

of the sample topography, 'Line Measure' which allows to measure different characteristic features of the sample surface. Image analysis allowed to infer various and important information about sample qualitative and quantitative features.

Both patterned mold topography and nanofilm thickness were characterized by means of AFM scanning. Imaging was performed with Veeco Innova Scanning Probe Microscope operating in tapping mode, with oxide-sharpened silicon probes (RTESPA-CP) at resonant frequency of about 300kHz. Thanks to AFM analysis it was possible both to measure the pillars height, the distance between adjacent pillars and the pillar diameters and to correlate these values with the photoresist spinning parameters. For measuring nanofilm thickness by AFM scanning instead, the films, free-suspended in water after sacrificial layer dissolution, were collected and dried onto a fresh silicon wafer. Thickness values were obtained by AFM cross-sectional analysis of nanofilm edge (SPMLab software version 7.20). The AFM scans were performed in three different areas of the same sample and on three different sample, in order to have a statistically significant data set.

### 2.2.2 SCANNING ELECTRON MICROSCOPE (SEM)

A SEM is a type of electron microscope that produces images of a sample by scanning it by means of a focused beam of electrons. The electrons interact with atoms in the sample, producing subsequently various signals that can be detected and that contain information about both the sample's surface topography and the composition. The electron beam is generally scanned in a raster scan pattern, and the beam's position is combined with the detected signal to produce an image. SEM can achieve resolution better than 1 nanometer. The most common mode of detection is by secondary electrons emitted by atoms excited by the electron beam. The number of secondary electrons is a function of the angle between the surface and the beam. By scanning the sample and detecting the secondary electrons, an image displaying the tilt of the surface is created. All samples

must be of an appropriate size to fit the specimen chamber and for conventional imaging in the SEM, specimens must be electrically conductive, at least at the surface, and electrically grounded to prevent the accumulation of electrostatic charge at the surface. Nonconductive specimens in fact tend to charge when scanned by the electron beam, and especially in secondary electron imaging mode, this causes scanning faults and other image artifacts. They are therefore usually coated with an ultrathin coating of electrically conducting material, deposited on the sample either by a low-vacuum sputter coating or by high-vacuum evaporation. An alternative to coating for some biological samples is to increase the bulk conductivity of the material by impregnation with osmium. Nonconducting specimens may be imaged uncoated using environmental SEM or low-voltage mode of SEM operation. For SEM, a specimen is required to be completely dry, since the specimen chamber is at high vacuum. Before SEM analysis, the samples were gold-sputtered (25 mA, 60 seconds) in order to supply a conductive coating to the specimen. SEM images were obtained by using a EVO MA15 SEM (Zeiss, Germany) equipped with $LaB_6$ source and working at 10kV accelerating voltage. The samples were scanned with different magnifications: 1.11 KX, 4.00 KX, 13.00 KX and 30.00 KX.

## 2.2.3. NANOFILM MECHANICAL PROPERTIES

The mechanical properties of the PLA nanosheets were characterized by the Strain-Induced Elastic Buckling Instability for Mechanical Measurement (SIEBIMM) technique. The SIEBIMM test is based on the buckling metrology and allows the calculation of Young's modulus for polymeric nanosheets **[51].** The elastic modulus can be calculated by measuring the buckling wavelength of the nanofilm collected on a mechanically compressed or stretched matrix. A free-standing PLLA nanosheet was collected from water onto a prestretched (3% strain of the original size) PDMS slab (1.5 cm x 4.0

cm). The configuration of the system used to perform SIEBIMM tests is shown in Figure 2.6, 2.7 and 2.8.

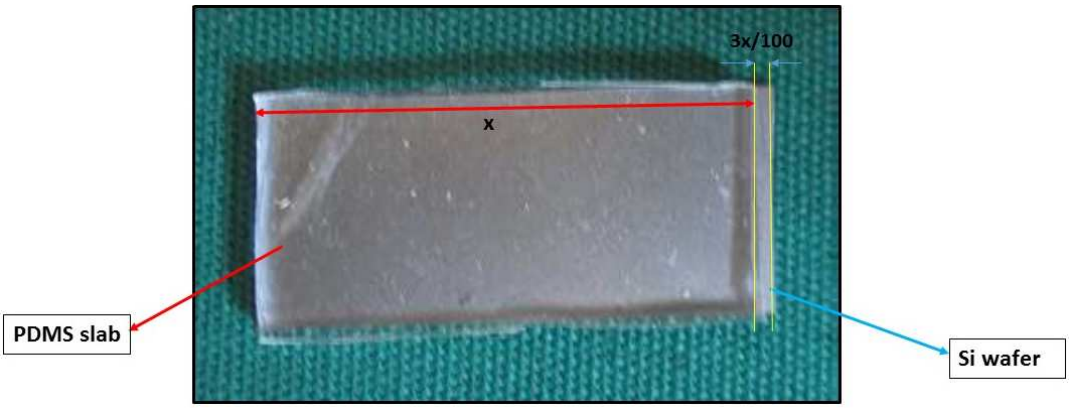


*Figure 2.6: PDMS slab with its of the original size on a silicon wafer having a length that is 103% strain of thePDMS slab length.*

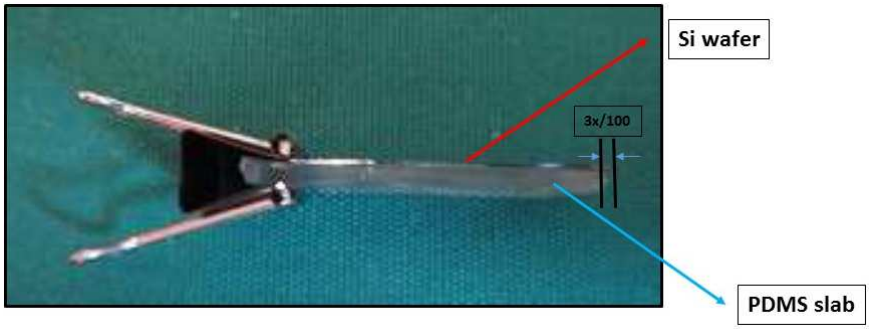


*Figure 2.7: Set up of the system used to perform the SIEBIMM test in the non-prestretched PDMS slab configuration, clamped at one side.*

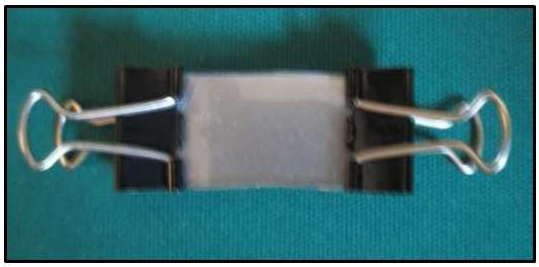

*Figure 2.8:* Set *up of the system used to perform the SIEBIMM test, after stretching the PDMS slab of the 3% respect to its original size, and clamping the correspondent side in order to keep it stretched.*

The prepared sample was dried in a desiccator overnight prior to the SIEBIMM test. Then, the strain of the PDMS substrate was relaxed, producing a relative compression of the PLA nanosheet and

generating a characteristic corrugation. The wavelength ($\lambda$) of the buckling pattern on the PLLA nanosheet was analyzed using an optical microscope (Hirox KH7700 digital microscope, Hirox Co Ltd., Tokyo, Japan ), equipped with a MX(G)-10C zoom lens and OL-700II objective lens. Three samples were analyzed and for each sample ten images relative to different areas and obtained with different magnifications were acquired.

Then, the Young's modulus ($E_{PLLA}$) of the PLLA nanosheet was obtainedby the following formula:

$$E_{PLLA} = 3 * \left(E_{PDMS} * (1 - (v_{PLLA})^2)\right)/(1 - (v_{PDMS})^2) * (\lambda/2 * \pi * h)^3$$

where:

$E_{PDMS} = 1.8MPa$ **Young's modulus of the PDMS slab**

$v_{PLLA} = 0.33$ **Poisson's ratio of PLLA nanosheet**

$v_{PDMS} = 0.5$ **Poisson's ratio of PDMS slab**

## 2.2.4. PERMEABILITY TESTS:

The permeability coefficient **K** of the porous nanofilms refers to water static capacity to pass through the membrane. Its evaluation is based on the measure of the liquid filtered through the nanofilm at different time-points. During the whole duration of the experiment the volume of the liquid, and consequently the pressure exerted on the nanofilm surface, was maintained constant. The evaluation of microporous nanofilms permeability found its theoretical motivations in the Darcy's law:

$$Q = (K * A/\mu) * ((P_a - P_b)/L)$$

where:

Q= flow rate

A=surface available for the transfer of the filtered fluid

μ=fluid viscosity

$P_b$,$P_a$ = pressures measured in correspondence of two sections

The flow rate Q was calculated by means of the following formula:

$$Q = (1/\rho) * (\Delta m/t)$$

$\Delta$m=liquid mass filtered during the time unit

$\rho$ =water density

$t$ =time duration to measure the liquid filtered through the nanofilm

$Q$ =flow rate

The pressure gradient is expressed by the following formula:

$$P_a - P_b = \Delta P = \rho * g * h$$

$\Delta P$ =hydrostatic pressure

$\rho$ =water density

$h$ =height of the hydrostatic volume exerting a constant pressure on the nanofilm surface.

*Figure 2.9: Lateral view of the set up of the system used to perform permeability tests.*

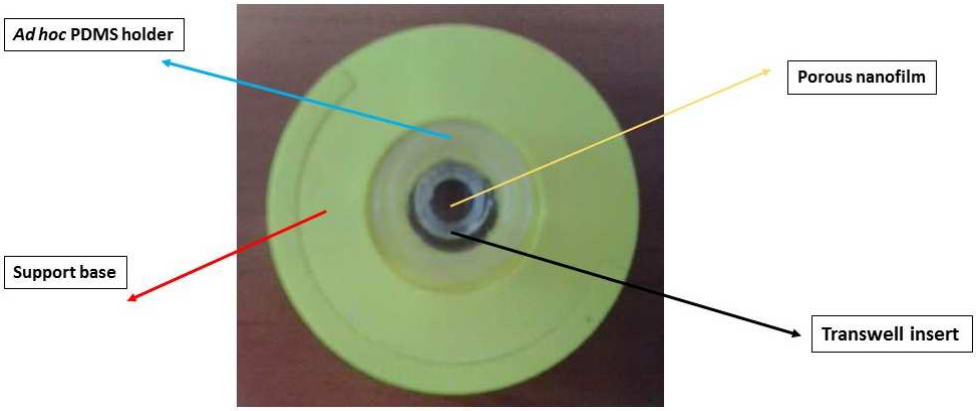


*Figure 2.10: Upper view of the set up of the system used to perform permeability tests.*

As shown in the Figure 2.9 and 2.10, the experimental set up used to perform permeability tests was composed of:

- A petri, where the liquid, filtered through the permeable nanofilm, was collected.
- An insert having an inner diameter of about 6.5 mm.
- An holder in PDMS which permitted hydraulic sealing and minimized fluid losses.
- A support base, shown in figure 2.10, designed by means of Solidworks, which allowed to maintain in a fixed and pre determined mutual position the nanofilm, respect to the petri, where the liquid filtered was collected.

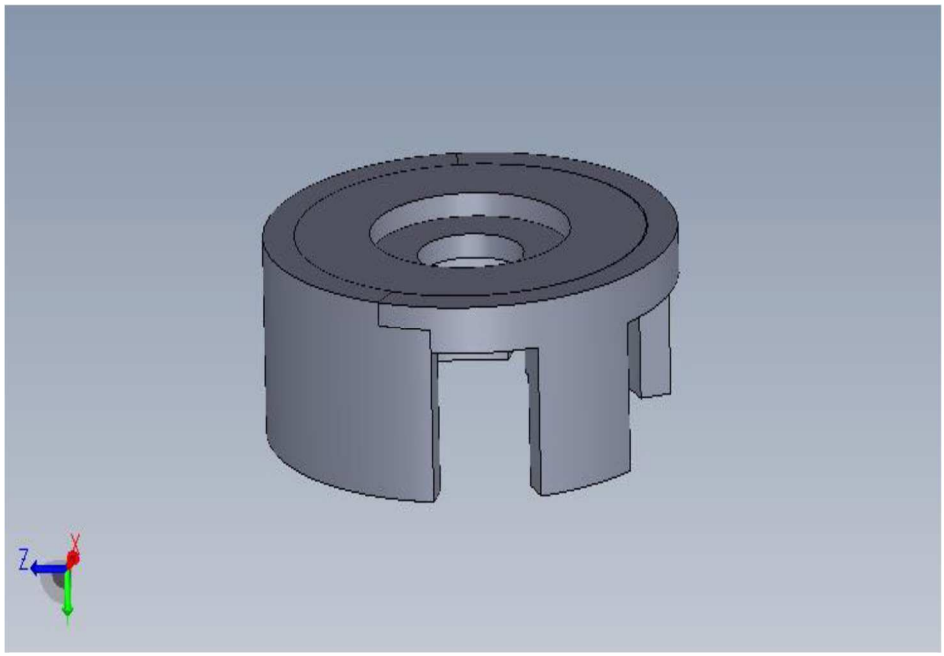

*Figure 2.11: Solidworks design of the support base.*

The procedure consisted of the following phases**:**

- The free-standing PLA nanofilm was collected from water on the insert.
- A thin layer of PDMS 1**:**9, reticulating overnight at room temperature, was introduced between the two holder parts in order to enhance hydraulic sealing and to minimize fluid losses.
- The insert was later embedded within a PDMS holder, having a proper shape and aimed at maximizing the hydraulic sealing.
- Finally, the nanofilm was chemically treated with ethanol (40*%* in water ), for 15 minutes before performing permeability tests.

Permeability was quantified by measuring the liquid filtered through the nanofilm at different time intervals, listed in Table 2.4**:**

| TIME INTERVAL [s] |
|---|
| 2 |
| 3 |
| 5 |
| 7 |
| 8 |
| 10 |
| 13 |
| 14 |
| 15 |
| 20 |
| 60 |

*Table 2.4: Time intervals relative to permeability tests.*

During the whole duration of the experiments, the pressure exerted by the volume of water, equal to 1 ml, was maintained constant. The time intervals were referred to a reference baseline, corresponding to the instant in which the fluid started to flow through the membrane.

## 2.2.5. STUDY OF FITC PS NANOPARTICLE PASSAGE THROUGH THE PERMEABLE NANOFILM:

Polystyrene Nanoparticles labelled with FITC-PS were used in order to investigate and characterize the passage of nanoparticles through the porous nanofilm. The choice of FITC-PS nanoparticles is related to the possibility to prepare and analyze samples using spectrophotometer. Moreover each sample can thus be analyzed step by step avoiding any problem of storage. FITC-PS (0.2 mg/ml in Eagle's Minimum Essential Medium, EMEM, containing 2% of FBS) of 200 nm in diameter were tested (Polysciences) because they are very easy to detect using a spectrofluoremeter. In order to prevent the possibility to form cluster in water, the Nanoparticles were dispersed in a 2% Fetal Bovine Serum (FBS) solution. FITC-PS nanoparticles are characterized by an excitation peak at about 441 nm and an emission peak at 486 nm.

The experimental procedure consisted of the following phases:

- FITC-PS nanoparticles were at firts sonicated for 10 min in order to make the solution homogeneous.
- Sonicated nanoparticles were later dispersed within an EMEM solution, containing 2% of FBS, at a concentration of 0.2 mg/ml.
- Before quantifying nanoparticle passage, the correlation between the absorbance and the concentration of the fluorescent compound was estimated in order to obtain the calibration curve. The calibration curve provides a linear fitting of the data, over a range of nanoparticle concentration from 0.001 mg/ml to 1 mg/ml (suspended in EMEM containing 2% of FBS).

The nanoparticle concentrations analyzed are listed in Table 2.5:

| NANOPARTICLES CONCENTRATION [mg/ml] |
|---|
| 1 mg/ml |
| 0.1 mg/ml |
| 0.05 mg/ml |
| 0.01 mg/ml |
| 0.005 mg/ml |
| 0.001 mg/ml |

*Table 2.5: Nanoparticle concentrations within the EMEM solution.*

The absorbance corresponding to the set of concentrations was evaluated by means of FLUOstar Omega spectrofluoremeter.

- PLA nanofilm was collected from water and blocked within the two parts of the Teflon holder. The holder was placed within a well of a 6-well multiwell plate. Volumes of 3 ml and 1 ml of EMEM solution containing 2% of Fetal Bovine Serum (FBS) were added below and above the nanofilm, respectively. The samples, having a volume of 100 μl, were taken and analyzed by means of FLUOstar Omega spectrofluoremeter, at different time-points, in order to quantify the amount of nanoparticles filtered through the nanofilm for different time intervals. The timetable followed to take the samples is listed in Table 2.6:

| SAMPLING TIMETABLE |
|---|
| 10 minutes |
| 30 minutes |
| 1 hour |
| 2 hours |
| 4 hours |
| 6 hours |

*Table 2.6: Timetable followed to analyze the samples.*

The analysis of the amount of nanoparticles passed through the nanofilm at different time-points

allowed to evaluate the transport kinetics of nanoparticles and to demonstrate the non deviousness of nanofilm pores. In particular, the percentage of nanoparticles passed, during a time interval, through the nanofilm respect to their initial concentration was correlated to the sampling time-points.

## 2.3 DESIGN OF A HOLDER FOR CELL CO-CULTURE:

A further step of the work consisted in the development of a Teflon holder, designed to allow cell co-culture in correspondence of the opposite sides of the porous polymeric nanofilm. Figure 2.11 shows the holder structure.

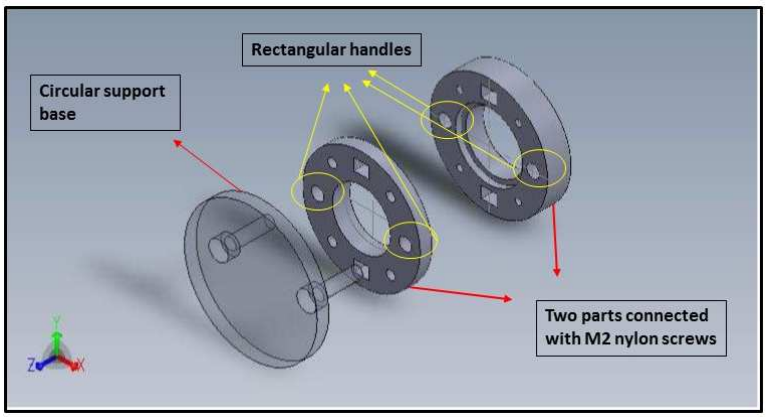


*Figure 2.11 Teflon holder.*

The holder was designed in order to be inserted within a well of a 6 well-plate and to allow membrane blocking. The holder was composed of the following constituents**:**

- A circular support base having two cylindrical columns, which allow holder insertion and blocking in a determined position**;**
- Two parts connected by means of M2 nylon screws**;**
- Two rectangular handles, which allow holder manipulation, repositioning and rotation.

## 2.4 CELL CULTURES:

### 2.4.1 INTESTINAL EPITHELIAL CACO-2 CELLS:

**Caco-2** is an established cell line of **heterogeneous human epithelial colorectal adenocarcinoma cells.** Although derived from a colon carcinoma, when cultured under specific conditions the cells become differentiated and polarized such that their phenotype, morphologically and functionally, resembles the enterocytes lining the small intestine. Caco-2 cells express tight junctions, microvilli, and a number of enzymes and transporters that are characteristic of such enterocytes. When looking at Caco-2 cell cultures microscopically, it is evident even by visual inspection that the cells are heterogeneous. Caco-2 celle are most commonly used not as individual cells, but as confluent monolayer. When cultured in this format, the cells differentiate to form a polarized epithelial cells monolayer that provides a physical and biochemical barrier to the passage of ions and small molecules. The Caco-2 monolayer is widely used across the pharmaceutical industry as an in vitro model of the human intestinal mucosa to predict the absorption of orally administered drugs.

### 2.4.2 CACO-2 CELLS CULTURE PROTOCOLS:

**Seeding protocol**

Caco-2 cells seeding protocol consisted of the following phases:

- Removal of the culture medium where Caco-2 cells were previously suspended
- Washing the cells with PBS in order to remove any residual of culture medium
- Addition of a volume of 3 ml of trypsin and further treatment in incubator at 37°C
- Cells Re-suspension in 3 ml of culture medium
- Centrifuging for 5 min at 900 rpm
- Supernatant removal
- Re-suspension in 1 ml of culture medium and subsequent cell counting by means of Trypan Blue

- Cell seeding, on the PLA nanofilm blocked within the holder, at a cell density of 40000 cells/cm², corresponding to 50000 cells cultured on each nanofilm.
- Addition of culture medium volumes of 5 ml and of about 1 ml respectively under and above the nanofilm.

EMEM culture medium was substituted with fresh medium every three days. Culture medium removal was performed by taking away the volume of medium which was at firts on the nanofilm and subsequently under the nanofilm. Volumes of 5 ml and 1 ml of fresh EMEM culture medium were added, respectively, below and above the nanofilm, respectively.

**Fixing with paraformaldehyde (PFA) protocol**

Paraformaldehyde is the polymerization product of formaldehyde with a typical degree of polymerization of 8-100 units. Once paraformaldehyde is depolymerized, the resulting formaldehyde is commonly used as a fixative for microscopy and histology. The fixing protocol by the use of PFA consists of the following phases:

- Removal of the culture medium where Caco-2 cells were suspended
- Washing the cells with PBS in order to remove any residual of culture medium
- Addition of volumes of PFA equal to 3 ml and 1 ml, respectively under and on the nanofilm blocked within the holder, at room temperature for 20 minutes.
- PFA removal.
- Washing the cells with PBS.
- Washing the cells with PBS a second time and leaving the cells dispersed in PBS at 4 °C.

**Cell staining**

- Cell permeabilization with 10 % Triton X-100 in PBS for 15 min.
- Rinsing two times with PBS, and saturation with 10 % goat serum (Invitrogen,Carlsbad, CA, USA) for 60 min.
- Samples were then provided with a staining solution constituted by red fluorescent phalloidin (λem 633 nm Sigma Aldrich), able to stain F-actin in red and DAPI to stain nuclei in blue.

- After 30 min of incubation at room temperature, the solution was removed and the samples were rinsed 3 times with PBS.
- Fluorescent samples were then inverted, mounted on glass slides, and imaged with a confocal fluorescence microscope (LSM 510 Meta, Carl Zeiss, Oberkochen, Germany).

# 3. EXPERIMENTAL RESULTS:

## 3.1 DEVELOPMENT OF POROUS NANOFILMS

### 3.1.1 MICROFABRICATION TECHNIQUE BASED ON SPIN COATING AND SALT LEACHING

The firts attempt to develop porous nanofilm was based on spin coating deposition on a silicon wafer, previously coated with a water-soluble sacrificial layer, of a polymeric solution containing a disperse phase of porogen particulate and further salt leaching in deionized water.

**POROGEN CHARACTERIZATION**

The porogen was characterized, in terms of quantification of grain size by SEM analysis of the porogen particles and the timing of the sifting phase was correlated to the resulting grain size. SEM analysis in fact allowed to estimate grain dimensions corresponding to the different sifting timing tested. Table 3.1 schematizes the correspondence between sifting timing and the resulting grain size.

| **SIFTING TIMING [min]** | 5 | 10 | 15 | 20 |
|---|---|---|---|---|
| **GRAIN SIZE [μm]** | 20 | 15 | 10 | 5-10 |

***Table 3.1*: *Schematization of the grain size as a function of different sifting timing.***

The grain size decreased by increasing the sifting timing and the minimum porogen size achieved was 5-10 μm. In principle, this size was considered acceptable for our purposes. In fact, we aimed at producing pores in the membrane with a diameter of 1-10 μm to assure a relatively high film porosity, but preventing at the same time the passage of entire cells through the membrane (a

maximum diameter of 10 µm was thus identified, for the pores).

## SEM ANALYSIS OF PLGA NANOFILMS

SEM images of PLGA nanofilms, obtained by spin coating and salt leaching, were acquired and analyzed (Figure 3.1 and Figure 3.2). In Figure 3.1 represents the areas correspondent to the edges of the nanofilm, whereas Figure 3.2 is relative to the central part of the membrane. It can be seen from the images that the external part of the membrane (close to its edge) is characterized by a certain porosity, with pore diameters mathing with the porogen size (5-10 µm). However, the central part of the nanofilm, corresponding to the majority of its area, is not porous.

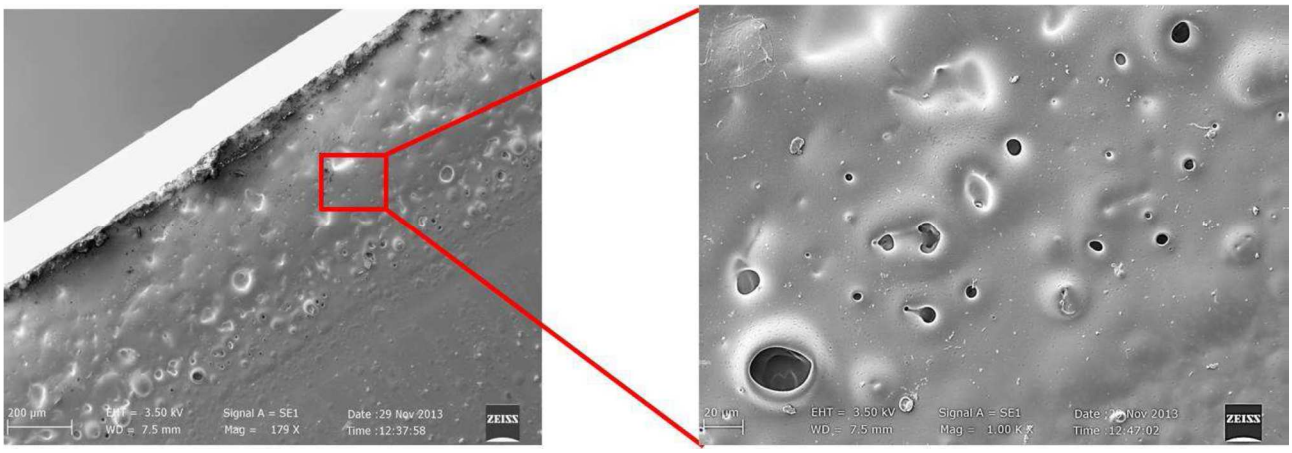


*Figure 3.1: SEM images of an area correspondent to one edge of the nanofilm.*

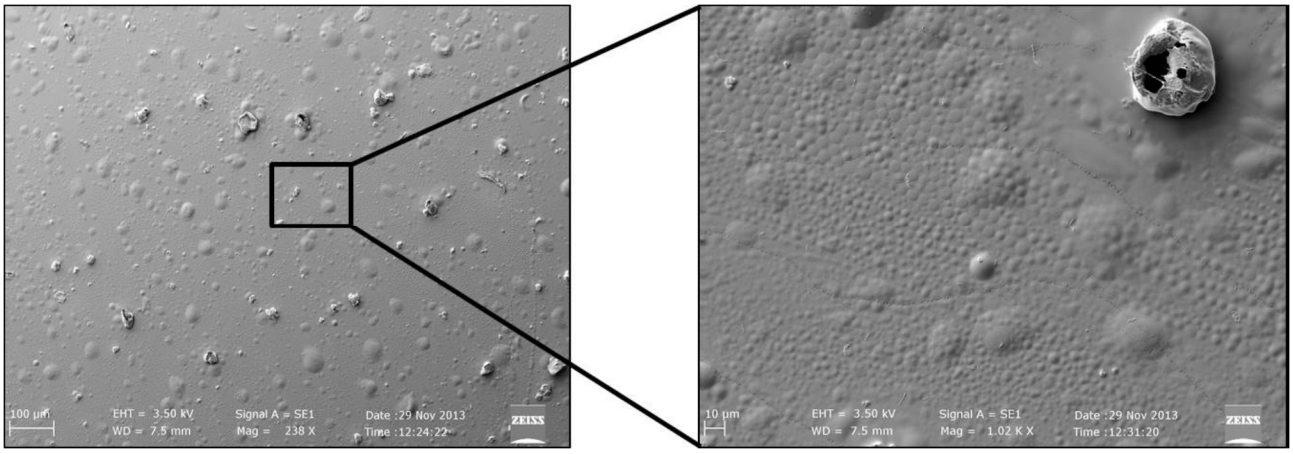


*Figure 3.2: SEM images of an area correspondent to the cental part of the nanofilm.*

In fact, the force due to viscous friction did not allow a homogeneous distribution of the porogen within the nanofilm, because of both porogen grain dimensions and of the nanometric thickness of the resulting film. Centrifugal force was responsible for a prevalent porogen distribution in correspondence of the nanofilm borders, which were consequently porous, whereas the central part of the film was not porous. A scheme representing the spin-coating deposition process and the inhomogeneous porogen distribution is reported in Figure 3.3.

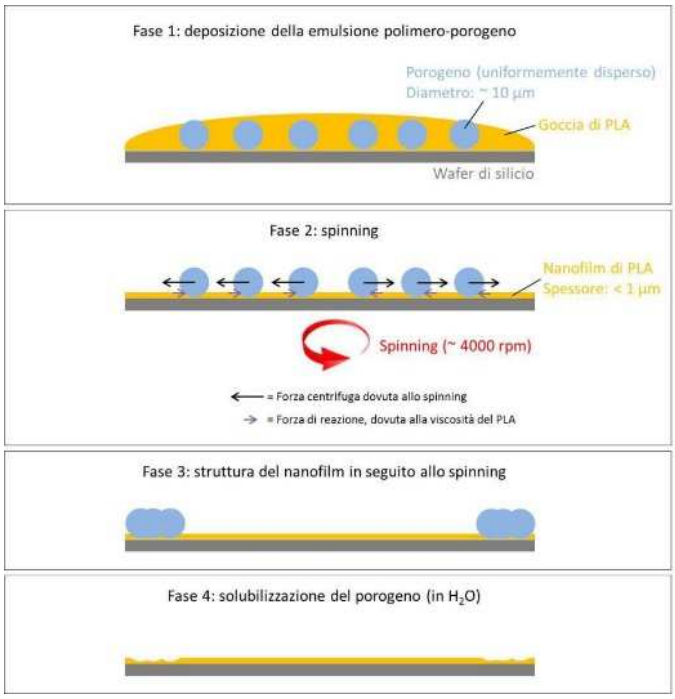


*Figure 3.3*: *Schematics concerning to porogen distribution before and after the spin-coating phase.*

Taking into account the above-mentioned considerations, the technique was not considered an effective means to achieve porous nanofilms. A possible solution to overcome this problem would be to reduce the grain size, thus allowing the porogen to lay completely inside the polymer solution during spin coating procedure. In the literature, there are some examples of porous polymeric films obtained by using salt leaching technique **[48, 49, 50]** (Figure 3.4 , 3.5)

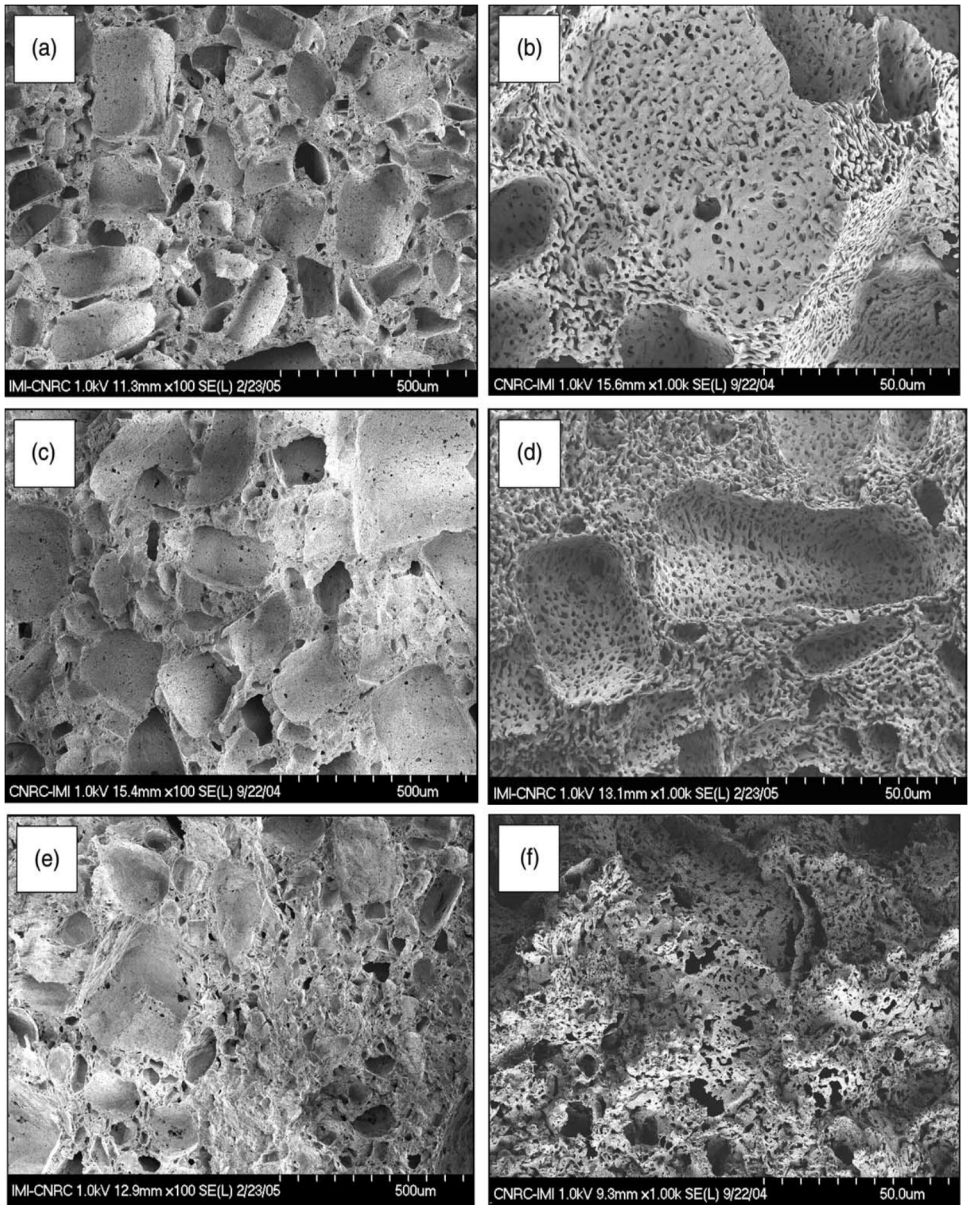


*Figure 3.4: SEM photomicrographs of PCL porous scaffolds generated after selective extraction of (a) and (b) 50% NaCl; (c) and (d) 60% NaCl; (e) and (f) 70% NaCl after dissolution of PEO and NaCl.*

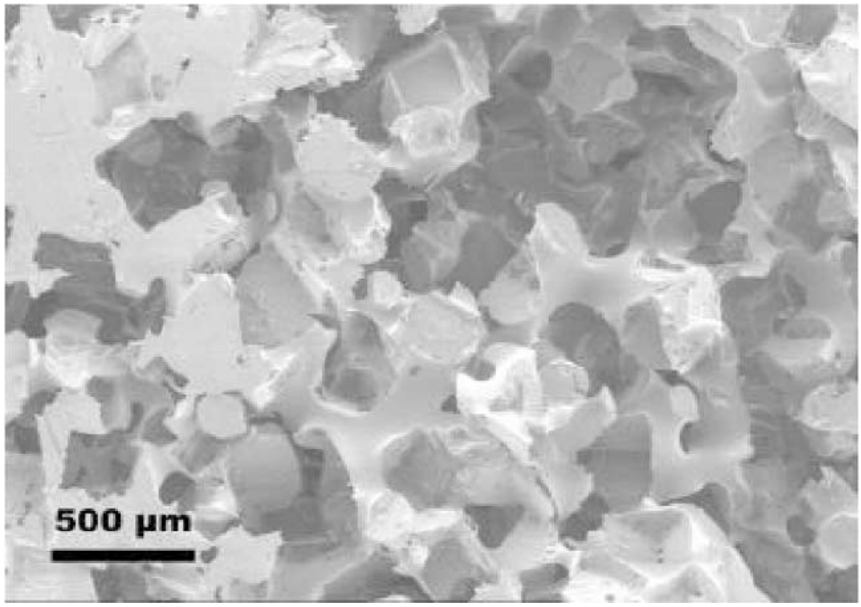


*Figure 3.5: SEM micrograph of a porous PDLLA structure prepared by compression moulding and salt leaching of mixtures of PDLLA and salt particles.*

However, these studies were focused on rather thick films, or the authors used really small porogens. For example *Tran et al* exploited the principles of crystallization to precisely control the porogen, sodium chloride, crystal sizes and thus obtained a reduction of salt particles diameter up to about 1.18 µm. Since we had not the possibility to achieve such porogen size with a simple and low cost technique (that is one of the Thesis purposes), we discarded salt leaching technique.

## 3.1.2 MICROFABRICATION TECHNIQUE BASED ON PHOTOLITHOGRAPHY

**Patterned mold characterization**

In order to establish the optimal photo-polymerization parameters, the topograpy of the patterned mold was evaluated for different spin coating parameters, by using AFM scans in tapping mode (Table 3.2):

| SPINNING SPEED [rpm] | PILLAR HEIGHT [□m] | DISTANCE BETWEEN PILLARS [μm] | PILLAR DIAMETER [μm] |
|---|---|---|---|
| **1500** | 1.50 ± 0.10 μm | 4.95 ± 0.45 μm | 4.94 ± 0.43 μm. |
| **2000** | 1.12 ± 0.15 μm | 3.75 ± 0.40 μm | 6.07 ± 0.35 μm. |
| **2500** | 0.85 ± 0.20 μm | 5.36 ± 0.43 μm | 4.49 ± 0.45 μm. |
| **3000** | 0.75 ± 0.17 μm | 4.90 ± 0.38 μm | 4.94 ± 0.30 μm. |

*Table 3.2: Patterned molds characterization for different spinning speeds.*

Table 3.2 shows that the pillar height decreased when the spin coating speed increased. This consideration is coherent with the theoretical expected results. This analysis allowed the selection of the most suitable spin-coating set of parameters in relation to the aim of the work. The selected spinning speed was 1500 rpm in order to obtain the highest pillars. This allowed to obtain pores with a uniform diameter (see the following sections ), because the membrane thickness to be used was lower than the height of the pillar in correspondence of which its diameter started to change, due to microfabrication defects (non perfect UV exposure, minimal but existing gap between the mask and the wafer during the exposure process, etc. )

Figure 3.6 shows the structure of the patterned molds, obtained by using such spin velocity.

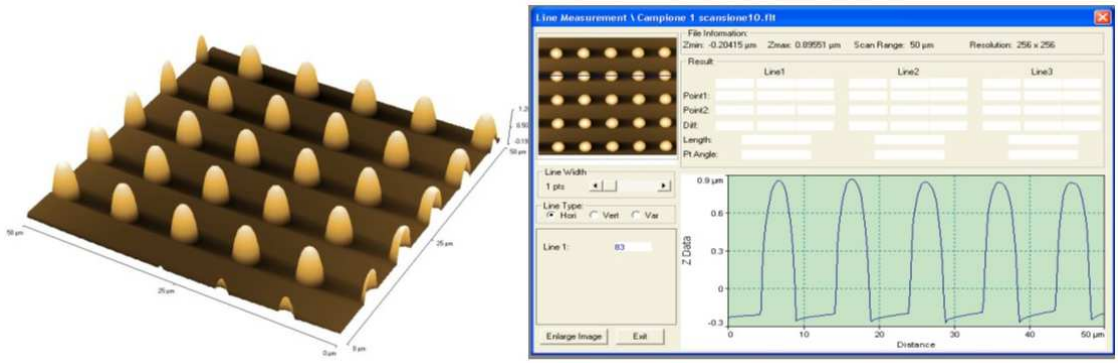


*Figure 3.6: 3D topography of a mold obtained by using 1500 rpm as spin velocity (left image ) and AFM height profile, corresponding to a line on the 2D scan (right image ).*

**Nanofilm characterization**

**Nanofilm thickness vs. spin coating speed**

Once the mold was obtained, the thickness of the resulting film was measured by AFM scanning in tapping mode, and correlated to the spin coating parameters in order to optimize film thickness (Table 3.3 and Figure 3.6 )

| SPINNING SPEED [rpm] | AVERAGE THICKNESS [µm] | STANDARD DEVIATION [%] |
|---|---|---|
| **3000** | 0,92 | 4,73 |
| **4000** | 0,71 | 8,40 |
| **5000** | 0,54 | 5,15 |
| **6000** | 0,44 | 6,08 |
| **7000** | 0,38 | 3,14 |

*Table 3.3: Nanofilm thickness characterization for different spinning speeds.*

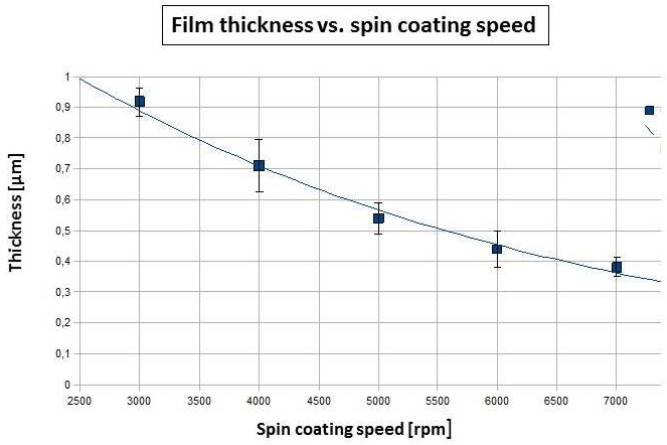


*Figure 3.7: Nanofilm thickness vs spin-coating speed.*

The results confirm the theoretical expectations**:** nanofilm thickness decreased as spin coating speed increased. This is due to the increase of centrifugal force for higher speeds. The results match with previous literature data, which report similar behaviours **[51,52].** Experimental results demonstrated that PLA spin-coating deposition on patterned molds, determined a resulting porous nanofilm which proved to be thicker than the non porous one obtained by spin coating on flat silicon wafers. The higher thickness of porous nanofilms, spin-coated on patterned molds, could be

reasonably due to the presence on the coated substrate of the cylidrical pillars, which obstructed PLA homogeneous deposition.

Moreover the correlation between the resulting film thickness and the spin coating speed can be fit with an exponential curve (Figure 3.5). It is possible to establish an analytical relation between spin coating speed and film thickness, in order to develop films with the desired thickness. Starting from this characterization, spin coating parameters were set at 6000 rpm for 20 seconds, in order to obtain nanofilms characterized by both a regular and pre-determined porous pattern. Moreover polymer film could be actuable by cardiac cells contractile force, thanks to the small thickness. The choice of these spin coating parameters allowed in fact to obtain nanofilms characterized by an average thickness of about **440 nm.**

**Nanofilm morphology and mechanical properties**

SEM images, obtained at different magnifications (Figures 3.6, 3.7 and 3.8), demonstrate the regular porous pattern characterizing PLA nanofilms.

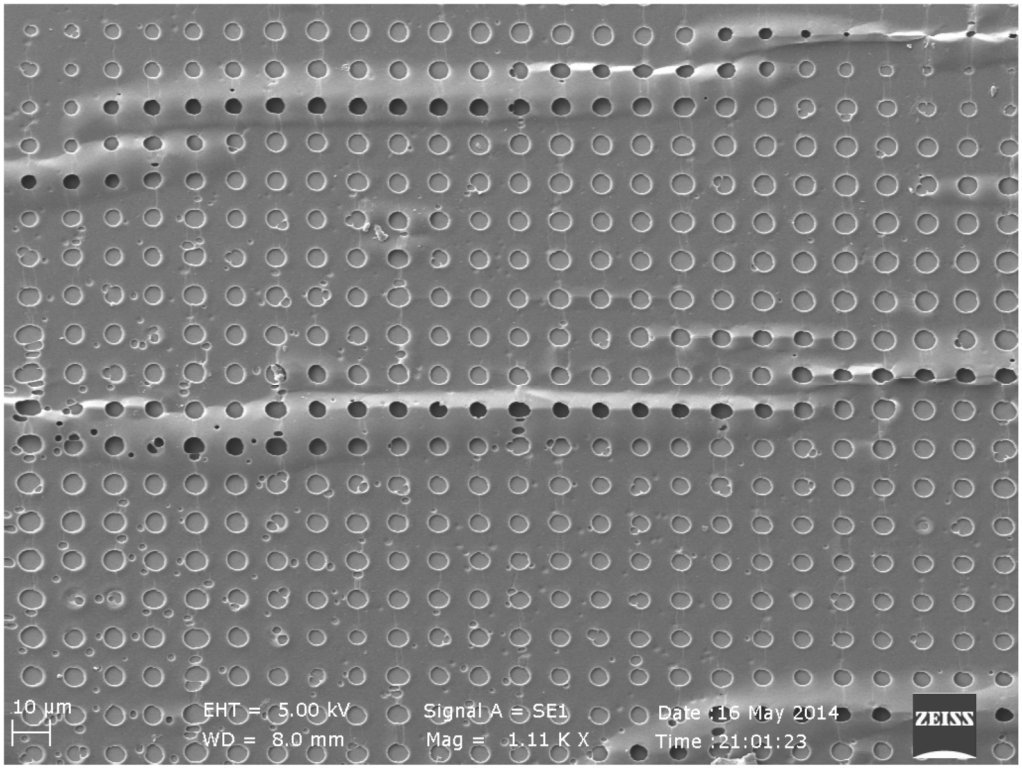


*Figure 3.8: SEM image of a porous nanofilm, obtained with 1.11 KX magnification.*

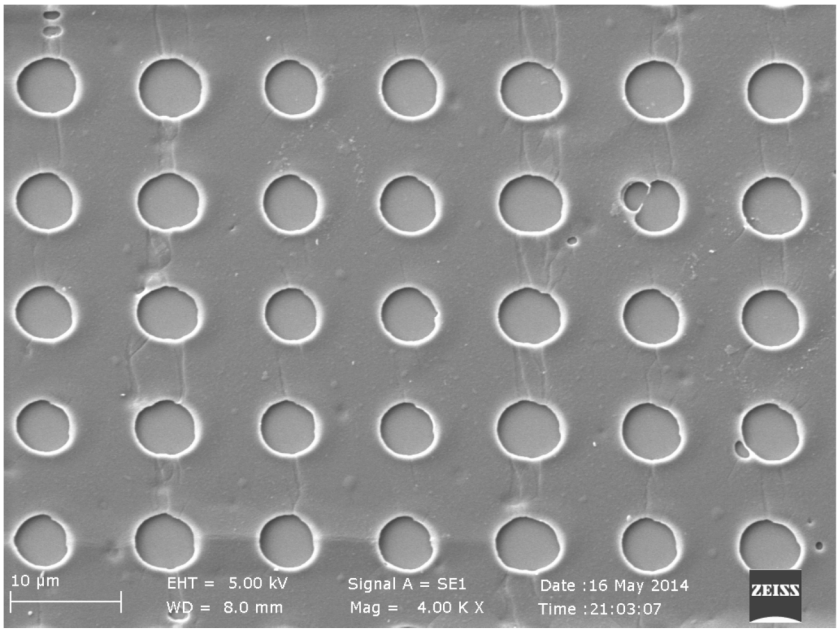


*Figure 3.9: SEM image of a porous nanofilm, obtained with 4.00 KX magnification.*

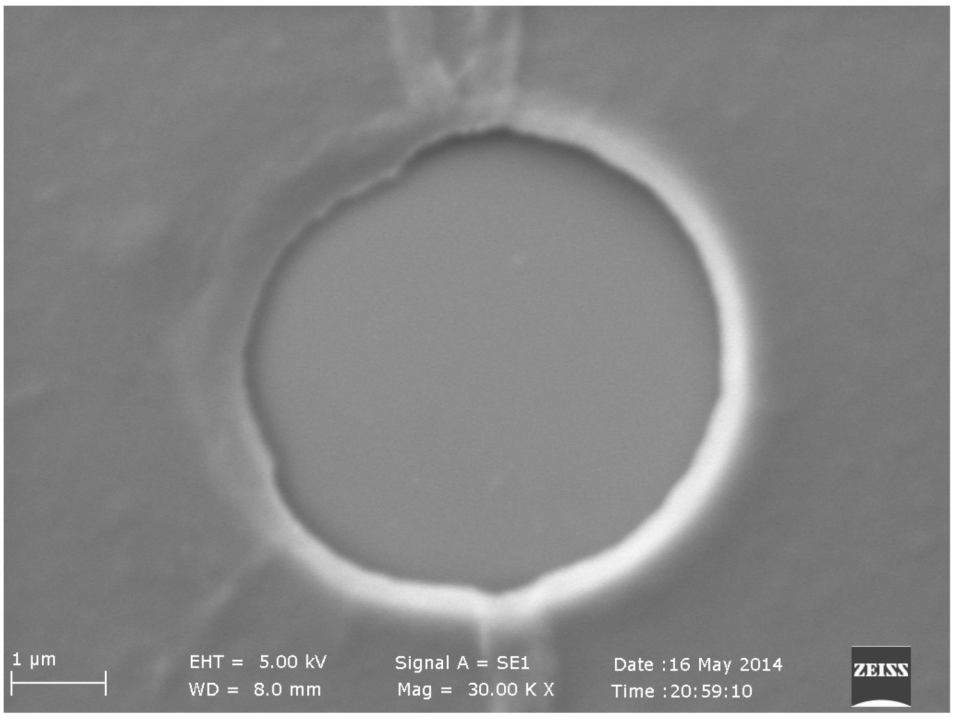


*Figure 3.10: SEM image of an individual pore obtained with 30.00 KX magnification.*

The SIEBIMM test, based on the buckling metrology, allowed the calculation of nanofilm Young's modulus. The Young's Modulus of the PLA porous nanosheets was estimated equal to $\mathbf{2.64 \pm 0.37}$

**GPa.** Figure 3.11 shows an Hirox image of the buckled nanofilm surface, with some measurements reported.

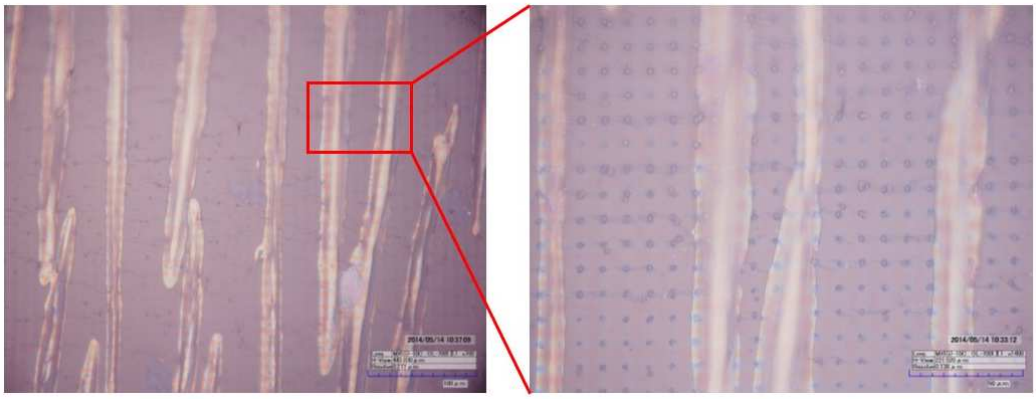

*Figure 3.11:HIROX image of the buckled nanofilm surface.*

The elastic modulus of highly elastic polymeric materials can vary from 7 MPa, up to 4 GPa in the case of stiffer polymers. In particular, PLA nanofilms have been already analyzed by *Fujie et al,* in terms of mechanical properties measured by SIEBIMM technique **[51].** Here, the authors showed that nanofilms with a comparable thickness to the ones we obtained, showed a Young's modulus of **6.6 ± 1.7 GPa.** The lower values we obtained are probably due to the presence of the pores.

The PLA porous nanofilms we obtained are rather stiff and resistant towards traction. In terms of mechanical properties, in the case of the application of a traction stress, porous PLA nanofilms showed a Young's modulus similar to the one of polycarbonate. Polycarbonate in fact is characterized by an elastic modulus, in the case of traction stress, of 2.38 GPa.

**Nanofilm permeability and passage tests**

Porous nanofilms were also characterized in terms of permeability, in order to study their usability as an interface system. They showed a rather high hydraulic permeability and good hydraulic withstanding. Nanofilm permeability coefficient was estimated equal to $4.75 * 10^{-10}$ **± 0.5 m².**

Furthermore, FITC-PS nanoparticle passage tests were performed on PLA nanofilms in order to demonstrate that, thanks to the non deviousness of its pores, the membrane allows the transit of nanoparticles. The purpose was to overcome the limitations characterizing current commercially

available membranes, which instead entrap nanoparticles within their structure, thus not allowing their passage. Figure 3.12 represents nanoparticles passage percentage, respect to the initial amount as a function of the different sampling time-points.

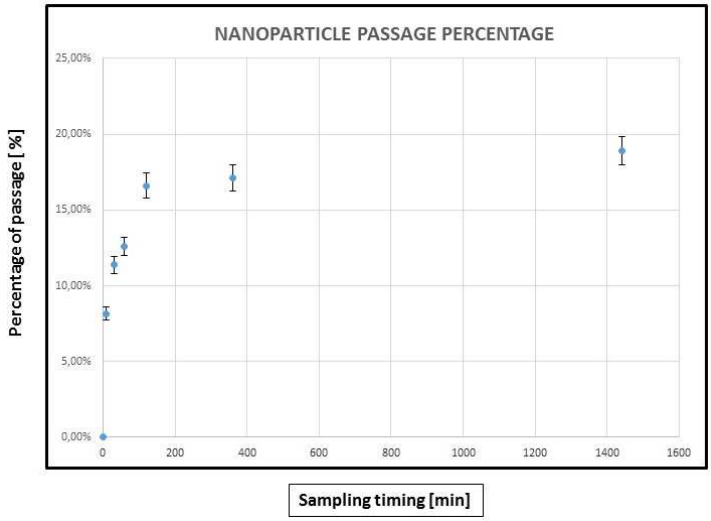


*Figure 3.12: Nanoparticles passage percentage as a function of different time-points.*

The data trend underlines that the nanoparticles, able to pass through the porous nanofilms, increased over time. The scatter graph consists of an initial tract characterized by a high increase of the nanoparticle passage rate through the nanofilm. After the initial transient, the data trend increases more slowly and tends to a plateau value, of about 19 % respect to the initial amount of FITC-PS. 24 h after the beginning of the experiments about 19 % of nanoparticles was filtered through the porous nanofilm. As the nanofilm is characterized by a theoretical porosity of about 20 %, 19 % of passage percentage means that almost all nanoparticles passed through the nanofilm pores and the residual quantity was not retained within the membrane, but was deposed on its surface. These results are very promising if compared to studies concerning nanoparticle passage through commercially available membranes. In the example proposed **[53]**, in fact the commercial membranes used almost did not allow the transit of nanoparticles, in static conditions, whereas in the case of dynamic passage studies, in presence of fluid flow, 24 h after the beginning of the experiments only 12 % of the original nanoparticle weight succeded in passing through the membrane.

## 3.2 CELL CULTURE RESULTS

### 3.2.1 INTESTINAL CACO-2 CELL CULTURE

In order to use the polymeric nanofilm as an interface for cell culture within a biohybrid system, preliminary tests of cell compatibility were performed. Caco-2 cells were cultured on PLA non porous nanofilms in order to evaluate the interaction and the compatibility between the cells and the material. The preliminary adhesion tests for Caco-2 cells cultured on PLA nanofilms revealed a good cell-material interaction, as demonstrated by the DAPI images, shown in Figure 3.13, 3.14 and 3.15.

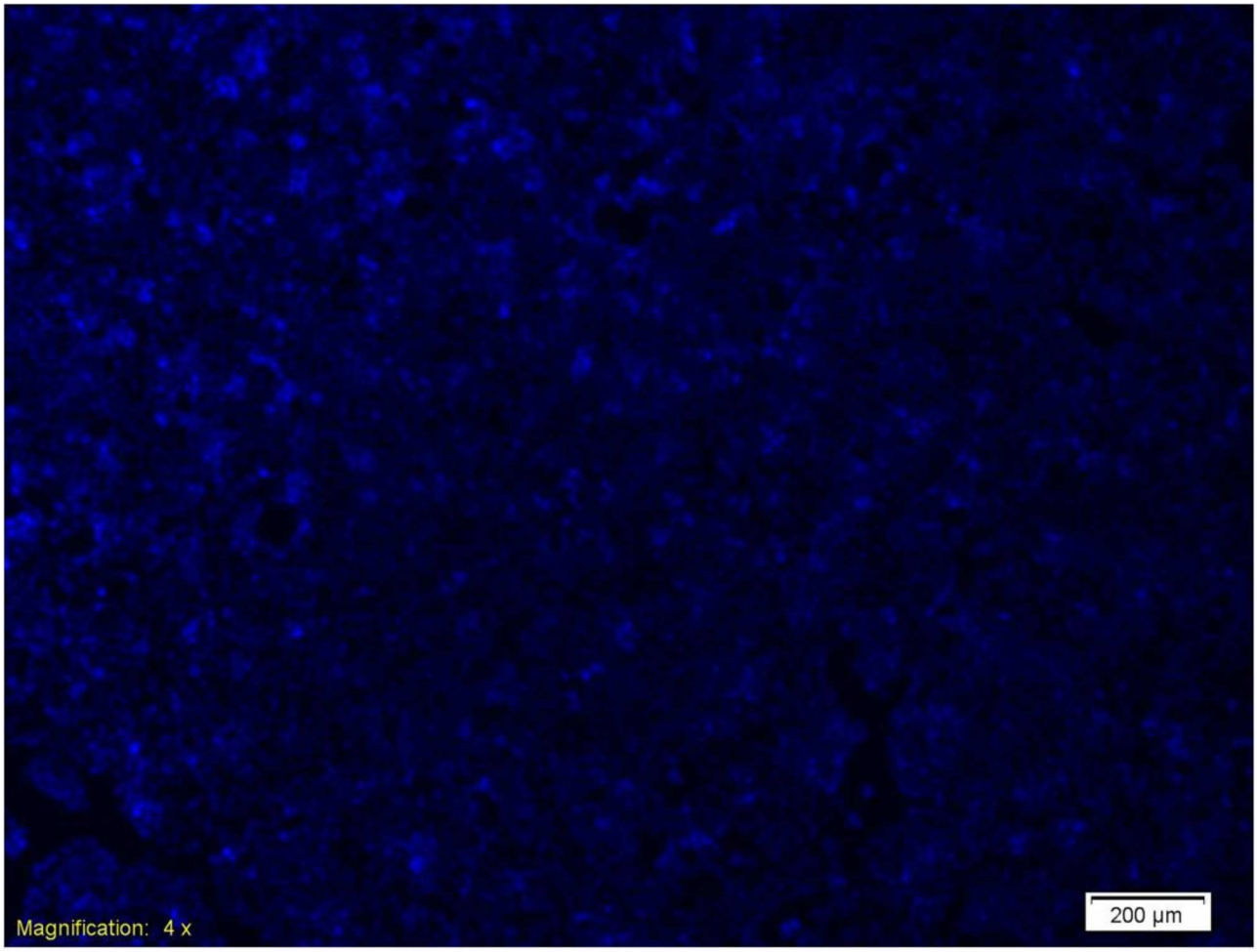


*Figure 3.13: DAPI* image (*cell nuclei*) *of Caco-2 cells cultured on PLA nanofilms (4x magnification).*

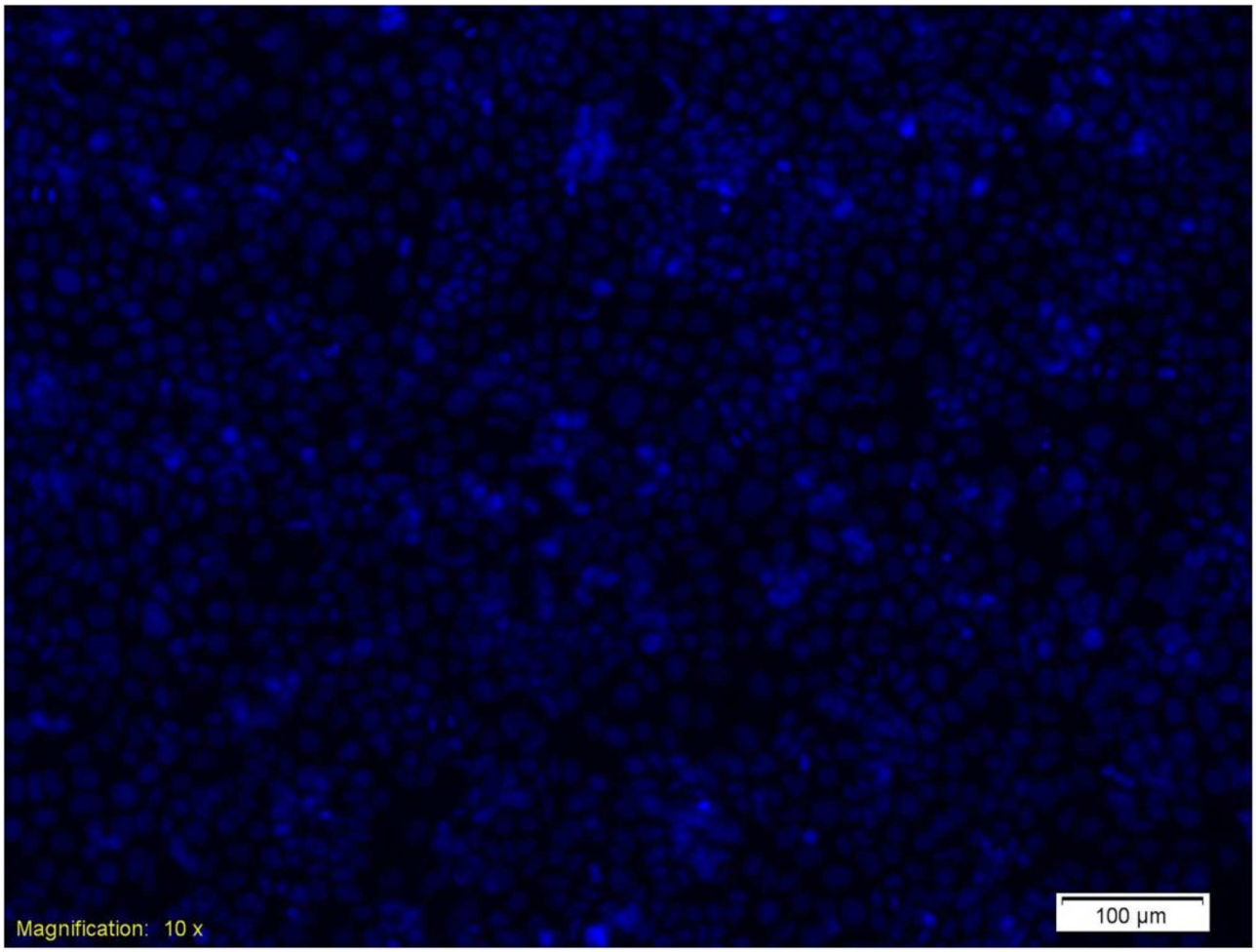


*Figure 3.14: DAPI image (cell nuclei )of Caco-2 cells cultured on PLA nanofilms (10x magnification).*

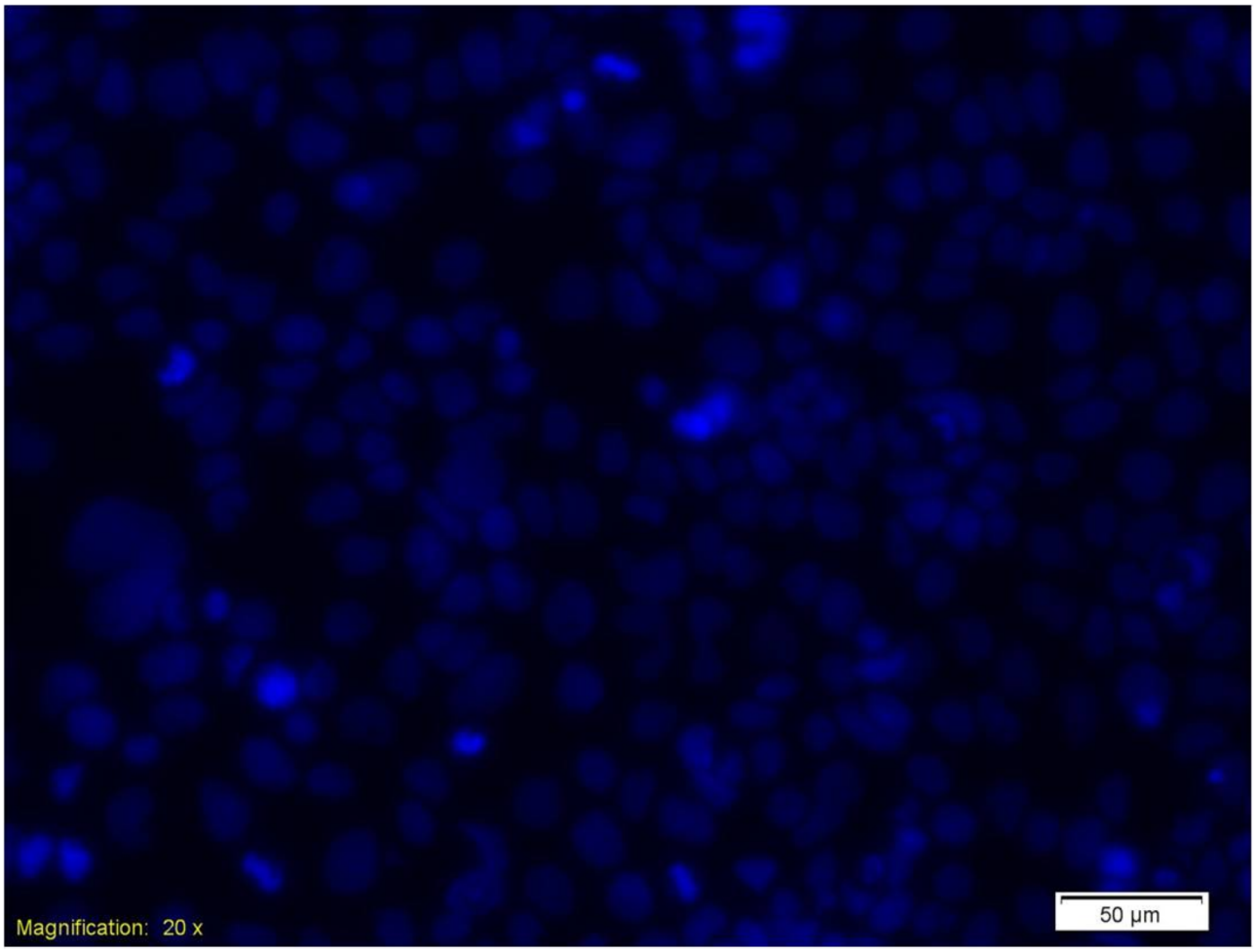


*Figure 3.15: DAPI image ( cell nuclei) of Caco-2 cells cultured on PLA nanofilms, (20x magnification).*

These preliminary results, demonstrated that PLA nanofilms show a good biocompatibility and allow Caco-2 cell adhesion on their surface, that is a pre-requisite for the final envisioned application. Caco-2 cell cultures on PLA nanofilms were viable for up to 7 days. The cells were fixed with PFA the third and the seventh day from the beginning of the culture to monitor the temporal development of cell growth and adhesion. Figure 3.16 shows the images relative to Caco-2 cell culture ( fixed with PFA on the third day of culture) seeded on PLA nanofilms, blocked within the Teflon holder.

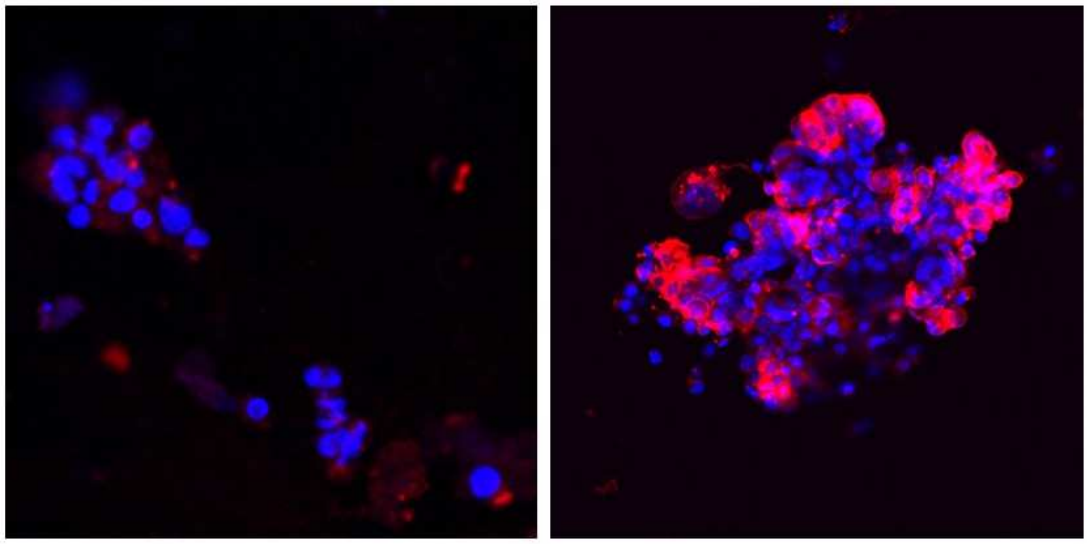

*Figure 3.16: Caco-2 cell culture on PLA nanofilms, blocked within a Teflon holder, fixed with PFA in correspondence of the third day of culture.*

Figures 3.17, 3.18 and 3.19 instead show Caco-2 cells, seeded on PLA nanofilms placed on a glass slide and fixed with PFA on the third day of culture.

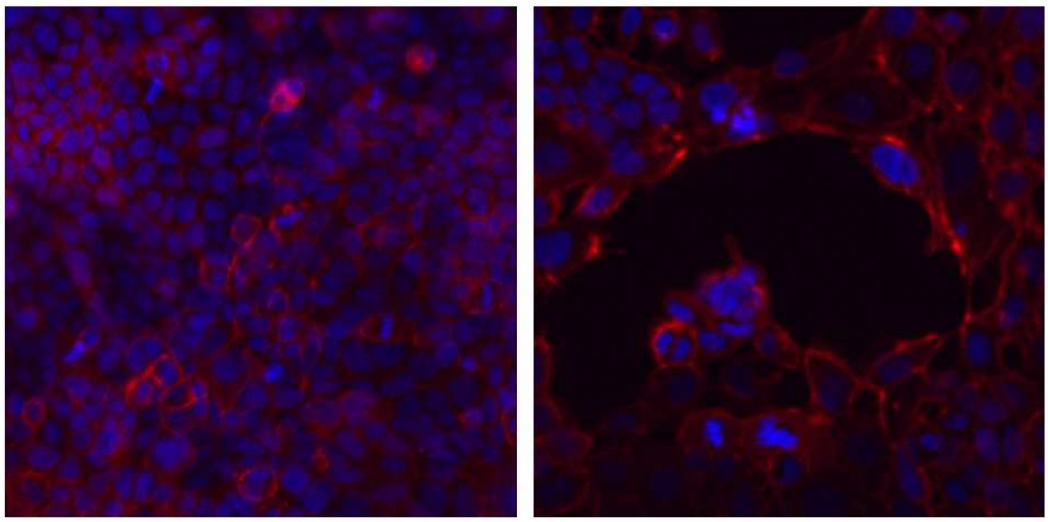

*Figure 3.17: Caco-2 cell culture on PLA nanofilms, placed on a glass slide and fixed with PFA on the third day of culture.*

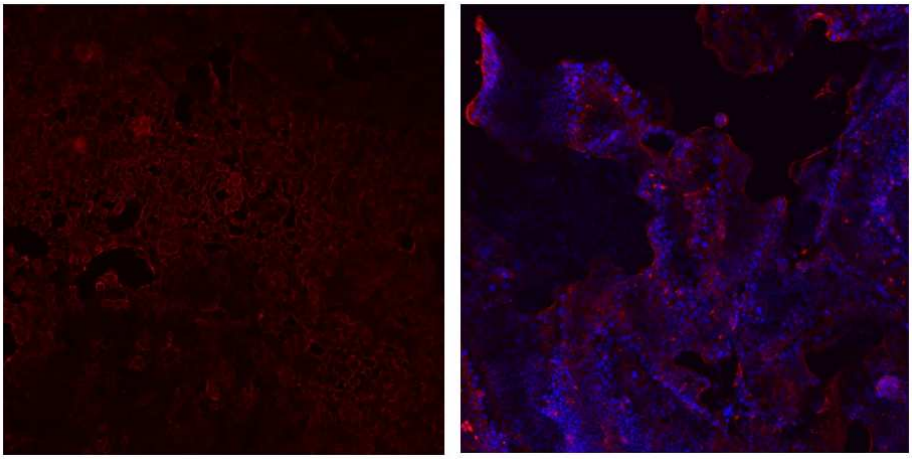

*Figure 3.18: Caco-2 cell culture on PLA nanofilms, placed on a glass slide and fixed with PFA on the third day of culture.*

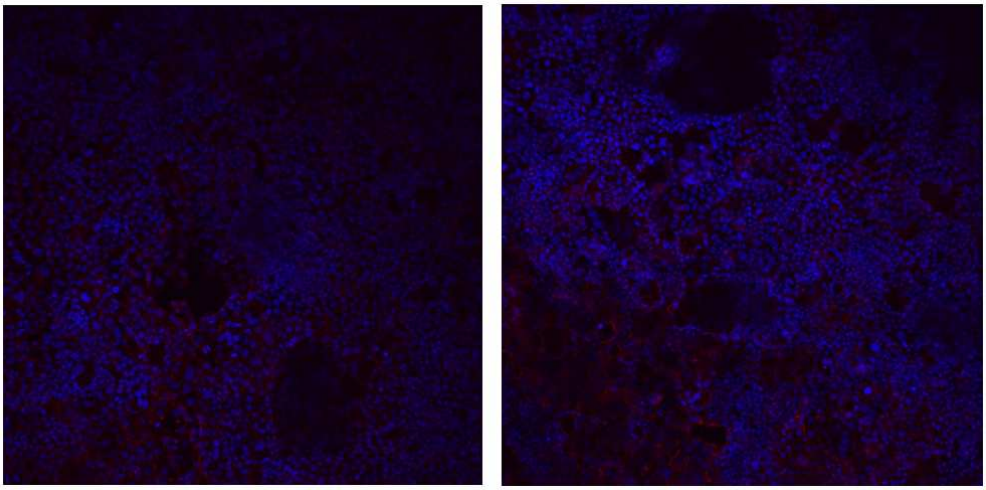

*Figure 3.19: Caco-2 cell culture on PLA nanofilms, placed on a glass slide and fixed with PFA on the third day of culture.*

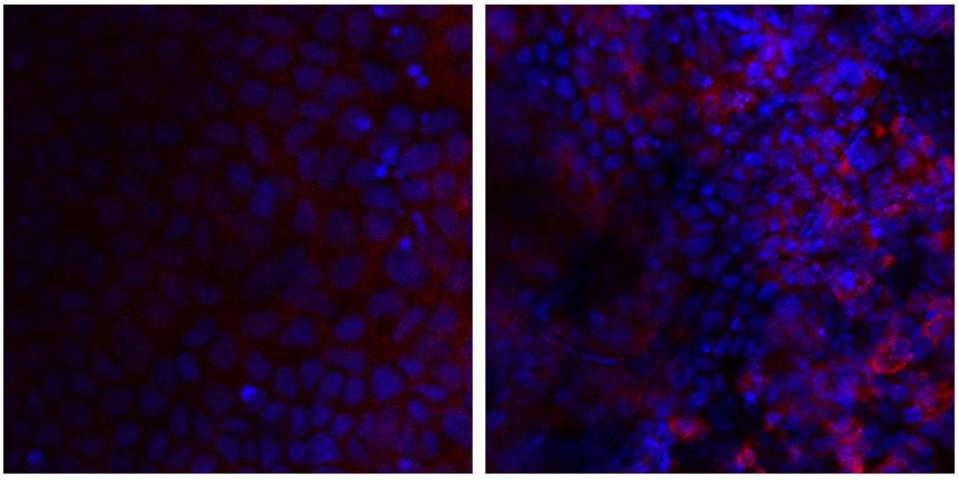

*Figure 3.20: Caco-2 cell culture on PLA nanofilms, placed on a glass slide and fixed with PFA on the seventh day of culture.*

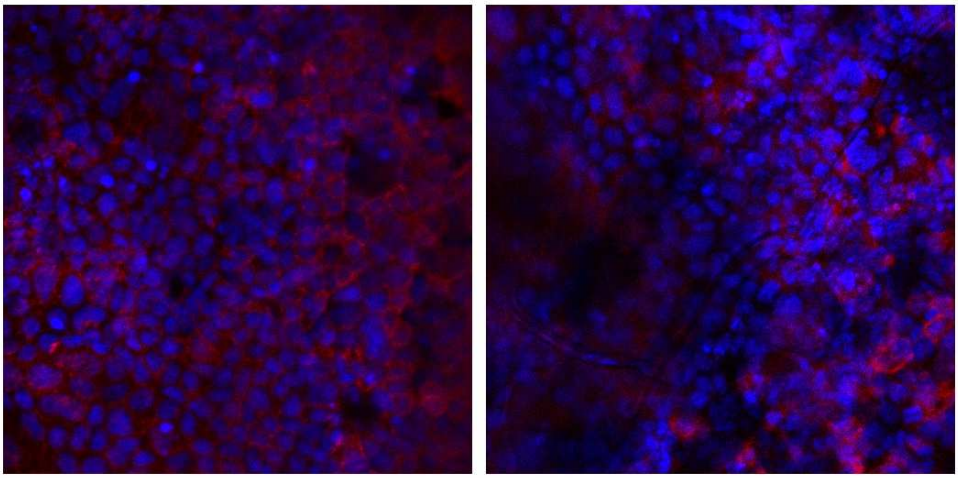

*Figure 3.21: Caco-2 cell culture on PLA nanofilms, placed on a glass slide and fixed with PFA on the seventh day of culture.*

The results showed a good biocompatibility of the porous PLA nanofilms with Caco-2 cell cultures, that were able to adhere, spread, proliferate and start to differentiate on such substrates.

# 4. CONCLUSIONS AND FUTURE DEVELOPMENTS

The objective of this Thesis was the design, development and characterization of a biomimetic system to be used as a tool to simulate the intestinal barrier *in vitro* and to study the cell-mediated passage of soluble and non soluble particles. The system proposed in this thesis is a biohybrid tool, based on a porous polylactid acid nano-membrane, which constitutes the interface between intestinal epithelial cell layer (Caco-2) and a self-beating muscle layer (mimed by cardiomyocites). The aim is to obtain an *in vitro* model, useful to test drugs, nanoparticles and other substances in terms of their toxic and/or therapeutic effects. The current research trend, aimed at engineering organs and tissues, is envisaged as a tool to complement or to replace tests on animals, widely used at present for toxicological analyses and drug testing. In addition to ethical concerns, *in vivo* tests are also characterized by long time durations and high costs, thus raising the need of effective *in vitro* alternatives. The *in vitro* tool developed in this thesis could be useful for the study of specific diseases related to dysfunctions in intestinal malabsorption mechanisms. The purpose of this work arises from the need to have a tool that allows to model the physiological and pathological features of the intestinal barrier and, on the other hand, the absorption mechanisms through it. Taking into account the intrinsic limitations of the traditional models and the lack of suitable technologies and procedures in the state-of-the-art, this works aims at:

**• developing a ultra-thin polymeric membrane provided with highly regular pores (conferring high permeability to the system) and showing high biocompatibility, thus allowing the culture of intestinal Caco-2 cells and cardiomyocytes. This will allow, with few evolutions of the device, to replace monocultures with co-cultures of these cells;**

**• developing a biohybrid tool that would be able, in future evolutions of the system, to generate contractile movements which simulate *in vitro* the peristalsis of the intestine occurring *in vivo*.**

The device proposed in this Thesis mimics the intestinal barrier as a permeable selective interface by the use of engineered porous PLA nano-membranes. Muscle cells would stretch the supporting

membrane and subsequently actuate the overall device, thanks to their capability to develop contractile active forces. The use of cardiac cells would allow to neglect and remove the problems due to the need of external electrical stimuli to contract the muscular fibers and subsequently to the integration of biocompatible electrodes in the system. The development of porous nanofilms allowed to create a permeable interface between two cell types, intestinal epithelial cells and mucle contractile cells. The purpose was to obtain nanofilms characterized by both a regular and pre-determined porous pattern and at the same time actuable by cardiac cells contractile force (thanks to the small thickness). PLA porous nanofilms, having a Young's modulus of **2.64 ± 0.37 GPa,** are thus rather stiff and resistant towards tractions stresses, they showed furthermore a rather high hydraulic permeability, good hydraulic withstanding and good permeability also to FITC-PS nanoparticle passage. Their capability to allow the passage of a consistent amount of nanoparticles, is an innovative potential in respect to the available commercial membranes, which entrap nanoparticles within and do not allow their transit in static conditions, without fluid flow. Preliminary tests of cell compatibility and viability were performed in order to evaluate the usability of the polymeric nanofilm as an interface for cell culture. The biological outcomes demonstrated that PLA nanofilms can be used within a biohybrid system, as they revealed a good cell-material interaction, allowing Caco-2 cells adhesion on their surface, that is a pre-requisite for the final envisioned application. The model proposed in this Thesis is a preliminary approach which tended to model the intestinal barrier in terms of both permeability and peristalsis. This prototype, could properly evolve in the future in a biomimetic device, more similar both from the morphological and from the functional point of view to the intestinal barrier *in vivo.* This could be obtaind by substituting self-beating cardiomyocytes with externally-stimulated smooth muscle cells, responsible for the actuation of the system, aimed at reproducing intestinal peristalsis. The co-culture of intestinal epithelial Caco-2 cells and muscle cells on the opposite sides of the interface nanofilm, could allow to perform passage studies of drugs and nanoparticles in both static conditions and in the presence of fluid flow, in order to evaluate the cell-mediated transit of

compounds, to perform drug screening and nanotoxicology studies.

## REFERENCES:


**[1]** E. Le Ferrec, C. Chesne, P. Artusson, D. Brayden, G. Fabre, P. Gires, F. Guillou, M. Rousset, W. Rubas, ML. Scarino. In vitro models of the intestinal barrier. The report and recommendations of ECVAM Workshop 46. European Centre for the Validation of Alternative Methods. Altern. Lab Anim. 29(6): 649-68 (2001).

**[2]** Liang-Shang L.Gan, Dhiren R. Thakker. Applications of the Caco-2 model in the design and development of orally active drugs: elucidation of biochemical and physical barriers posed by the intestinal epithelium. Advanced Drug Delivery Reviews. 23: 77-98 (1997).

**[3]** X. T. Zeng, L. Yu, P. Li, H. Dong, Y. Wang, Y. Liu, C. Ming Li. On-chip investigastion of cell-drug interactions. Advanced Drug Delivery Reviews. 65: 1556-1574 (2013).

**[4]** D. Huh, B. D. Matthews, A. Mammoto, M. Montoya-Zavala, H. Y. Hsin, D. E. Ingber. Reconstituting Organ-Level Lung Functions on a Chip. Science. 328 (5986): 1662-1668 (2010).

**[5]** C. Lochovsky, S. Yasotharan, A. Vagaon, D. Lidington, J. Voigtlaender-Bolz, S-S. Bolz, A Günther. Artery-on-a-chip. Lab Chip. 10 (18): 2341-2349 (2010).

**[6]** J. Park, H. Koito, A. Han. Microfluidic compartimentalized co-culture platform for CNS axon myelination research. Biomed Microdevices. 11 (6): 1145-1153 (2009).

**[7]** L. You, S. Temiyasathit, P. Lee, C. H. Kim, P. Tummala, W. Yao, W. Kingery, A. M. Malone, R. Y. Kwon, C. R. Jacobs. Osteocytes as Mechanosensors in the Inibition of Bone Resorption Due to Mechanical Loading. Bone. 42(1): 172-179 (2008).

**[8]** R. Sudo, S. Chung, IK. Zervantonakis, V. Zickerman, Y. Toshimitsu, LG. Griffith, RD. Kamm. Transport-mediated angiogenesis in 3D epithelial cocoltures. FASEB J. 23 (7): 2155-2164 (2009).

**[9]** T. Poghosyan, S. Gaujoux, V. Vanneaux, P. Bruneval, T. Domet,S. Lecourt, M. Jarraya, R. Sfeyr, J. Larghero, P. Cattan. *In vitro D*evelopment and Characterization of a Tissue- Engineered Conduit Resembling
Esophageal Wall Using Human and Pig Skeletal Myoblast, Oral Epithelial Cells, and Biologic Scaffolds. Tissue Engineering: Part A. 19: 2242-2252 (2013).

**[10]** S. Giusti, T. Sbrana, M. La Marca, V. Di Patria, V. Martinucci, A. Tirella, A. Ahluwalia. A novel dual-flow bioreactor simulates increased fluorescein permeability in epithelial tissue barrier. Biotechnology Journal. 9 (2014).

**[11]** Sonntag, F. et al. Biotechnology Journal. 148, 70-75 (2010).

**[12]** G. T. Vladisavlijevic, N. Khalid, M.A. Neves, T. Kuroiwa, M. Nakajima, K. Uemura, S. Ichikawa, I. Kobayashi. Industrial lab-on-a-chip: Design, applications and scale-up for drug discovery and delivery. Advanced Drug Delivery Reviews. 65: 1626-1663 (2013).

**[14]** K. Bhradriraju, C. S. Chen. Engineering cellular micro-environments to impove cell-based drug testing. Drug Discov. Today. 7 (11): 612-620 (2002).

**[15]** H. Vandenburgh, J. Shansky, F. Benesch-Lee, V. Barbata, J. Reid, L. Thorrez, R. Valentini, G. Crawford. Drug-screening platform based on the contractility of tissue-engineered muscle. MUSCLE & NERVE. 8: 438-447 (2008).

**[16]** Silverthon D. U., Fisiologia. Un approccio integrato. Milano: Casa Editrice Ambrosiana, 2007.

**[17]** F. Scaldaferri, L. Lopetruso, S. Pecere, V. Gerardi, F. Forte, A. Tortora, G. Ianiro, A. Gasbarrini. La barriera intestinale: nuove acquisizioni e approcci terapeutici. (2011)

**[18]** S. Sant, S. L. Tao, O. Z. Fisher, Q. Xu, N. A. Peppas, A. Khademhosseini. Microfabrication technologies for oral drug delivery. Advanced Drug Delivery Reviews. 64: 496-507 (2012).

**[19]** L. Wang, S. K. Murthy, W. H. Fowle, G. A. Barabino, R. L. Carrier. Influence of micro-well biomimetic topography on intestinal epithelial Caco-2 cell phenotype. Biomaterials. 30: 6825-6834 (2009).

**[20]** L. Wang, S. K. Murthy, G.A. Barabino, R. L. Carrier. Synergic effects of crypt-like topography and ECM proteins on intestinal cell behaviour in collagen based membranes. Biomaterials.31: 7586-7598 (2010).

**[21]** R. C. Gunawan, E. R. Choban, J. E. Conour, J. Silvestre, L. B. Schook, H. R. Gaskins, D. E. Leckband, P.J.A. Kenis. Regiospecific control of protein expression in cells cultured on two-component counter gradients of extracellular matrix proteins. Langmuir. 21: 3061-3068 (2005).

**[22]** B. V. Slaughter, S.S. Khurshid, O.Z. Fisher, A. Khademosseini, N.A. Peppas. Hydrogels in regenerative medicine. Adv. Mater. 21:3307-3329 (2009).

**[23]** S.Sant, M. J. Hancock, J. P. Donnelly, D. Iyer, A. Khademosseini. Biomimetic gradient hydrogels for tissue engineering. Can. J. Chem. Eng. 88: 899-911 (2010).

**[24]** M. P. Lutolf. Spotlight on hydrogels. Nat. Mater. 8: 451-453 (2009).

**[25]** N. A. Peppas, Y. Huang, M. Torres-Lugo, J.H. Ward, J. Zhang. Physicochemical, foundations and structural design of hydrogels in medicine and biology. Annu. Rev. Biomed. Eng. 2:9-29 (2000).

**[26]** N. A.Peppas, J. Z. Hilt, A. Khademosseini, R. Langer. Hydrogels in biology and medicine: from molecular principles to bionanotechnology. Adv. Mater. 18: 1345-1360 (2006).

**[27]** J. H. Sung, J. Yu, D. Luo, M. L. Shuler, J.C March. Microscale 3-D hydrogel scaffold for biomimetic gastrointestinal (GI) tract model. Lab Chip. 11: 389-392 (2011).

**[28]** GJ. Mahler, MB. Esch, RP. Glahn, ML. Shuler. Characterization of gastrointestinal tract microscale cell culture analog used to predict drug toxicity. Biotechnol. Bioeng. 104(1): 193-205 (2009).

**[29]** M. B. Esch, J. H. Sung, J. Yang, C. Yu, J. Yu, J. C. March, M. L. Shuler. On chip porous polymer membranes for integration of gastrointestinal tract epithelium with microfluidic 'body-on-a-chip' devices. Biomed Microdevices. 14: 895-906 (2012).

**[30]** S. H. Choi, M. Nishikawa, A. Sakoda, Y. Sakai. Feasibility of a simple double-layered cocolture system incorporating metabolic processes of the intestine and liver tissue: application to the analysis of benzo a pyrene toxicity. Toxicol. Vitr. 18: 393-402 (2004).

**[31]** Y. Y. Lau, Y.-H. Chen, T.-t Liu, C. Li, X. Cui, R. E. White, K.-C. Cheng. Evaluation of a novel in vitro caco-2 hepatocyte hybrid system for predicting in vivo oral bioavailability. Drug Metab. Dispos. 32:937-942 (2004).

**[32]** G. J. Mahler, M. L. Shuler, R. P. Glahn. Characterization of Caco-2 and HT29-MTX cocoltures in an in vitro digestion/cell culture model used to predict iron bioavailability. J. Nutr. Biochem. 20: 494-502 (2009).

**[33]** Y. Imura, Y. Asano, K. Sato, E. Yoshimura. A microfluidic system to evaluate intestinal absorption. Anal. Sci. 25: 1403-1407 (2009).

**[34]** K.-J. Jang, K.-Y. Suh. A multi-layer microfluidic device for efficient culture and analysis of renal tubular cells. Lab Chip. 10: 36-42 (2010).

**[35]** K.-J. Jang, H. S. Cho, D. H. Kang, W. G. Bae, T. -H.Kwon, K. -Y.Suh. Fluid shear-stress-induced traslocation of aquaporin-2 and reorganization of actin cytoskeleton in renal tubular epithelial cells. Integr. Biol. 3: 134-141 (2011).

**[36]** H. Kimura, T. Yamamoto, H. Sakai, Y. Sakai, T. Fujii. An integrated microfluidic system for long-term perfusion culture and on-line monitoring of intestinal tissue models. Lab Chip. 8: 741-746 (2008).

**[37]** Y. Imura, Y. Asano, K. Sato, E. Yoshimura. A Microfluidic System to Evaluate Intestinal Absorption. Analytical Sciences. 25: 1403-1407 (2009).

**[38]** R. P. Brown, M. D. Delp, S. L. Lindstedt, L. R. Rhomberg, R. P. Beliles. Physiological parameter values for phisiologically based pharmacokinetic models. Toxicol. Ind. Heal. 13: 407-484 (1997).

**[39]** R. Khamsi.Labs on a chip meet the stripped down rat. Nature. 435: 12-13 (2005).

**[40]** P. Stenberg, K. Luthman, P. Artursson. Virtual screening of intestinal drug permeability. Journal of Controlled Release. 65: 231-243 (2000).

**[41]** M. Kansy, F. Senner, K. Gubernator. Physiochemical high throughput screening: parallel artificial membrane permeation assay in the description of passive absorption processes. J. Med. Chem. 41: 1007-1010 (1998).

**[42]** D.-C Kim, P.S. Burton, R.T. Borchardt. A correlation between the permeability characteristics of a series of petides using an in vitro cell culture model (Caco-2) and those using an in situ perfused rat ileum model of the intestinal mucosa. Pharm. Res. 10: 1710-1714 (1993).

**[43]** M. E. Lane, C.M. ODriscoll, O.I. Corrigan. The relationship between rat intestinal permeability and hydrophilic probe size. Pharm. Res. 13: 1554-1558 (1996).

**[44]** AY. Hsiao, YS. Torisawa, YC Tung, S. Sud, RS. Taichman, KJ. Pienta, S. Takayama. Microfluidic system for formation of PC-3 prostate cancer co-culture spheroids. Biomaterials. 30 (16): 3020-3027 (2009).

**[45]** N. Ferrel, R.R. Desai, A.J. Fleischman, S. Roy, H.D.Humes, W. H. Fissel. A microfluidic bioreactor with integrated transepithelial elictrical resistance (TEER) measurement electrodes for evaluation of renal epithelial cells. Biotechnol. Bioeng. 107:707-716 (2010).

**[46]** KR. Groschwitz, SP. Hogan. Intestinal barrier function: molecular regulation and disease pathogenesis. J Allergy Clin Immunol. 124(1):3-20 (2009).

**[47]** J. M. DeSesso, C. F. Jacobson. Anatomical and physiological parameters affecting gastrointestinal absorption in humans and rats. Food and Chemical Toxicology. 39: 209-228 (2001).

**[48]** J. Reigner, M. A. Huneault. Preparation of interconnected poly(3-caprolactone) porous scaffolds by a combination of polymer and salt particulate leaching. Polymer. 47 : 4703–4717 (2006).

**[49]** Q. Hou, D. W. Grjpma, J. Feijen. Porous polymeric structures for tissue engineering prepared by a coagulation, compression moulding and salt leaching technique. Biomaterials 24 : 1937–1947 (2003).

**[50]** Tran RT., Naseri E., Kolasnikov A, Bai X., Yang J. A new generation of sodium chloride porogen for tissue engineering. Biotechnol Appl Biochem. 58 : 335-44 (2011).

**[51]** T. Fujie, L. Ricotti, A. Desii, A.Menciassi, P. Dario, V.Mattoli. Evaluation of substrata effect on cell adhesion properties using freestanding poly (L-lactic acid) nanosheets. Langmuir. 27 : 13173-82 (2011).

**[52]** L. Ricotti, S. Taccola, V. Pensabene, V. Mattoli, T. Fujie, S. Takeoka, A. Menciassi, P. Dario. Adhesion and proliferation of skeletal muscle cells on single layer poly (lactic acid) ultra-thin films. Biomed Microdevices. 12 : 809-819 (2010).

**[53]** T. Sbrana, Fluidic systems design for physiologically relevant in-vitro models, University of Pisa, XXIV cycle, 2011

**[54]** Scriven, LE, Physics and applications of dip coating and spin coating. *MRS proceedings*, 121 (1988)

**[55]** Jaeger, Richard C. (2002). "Lithography". Introduction to Microelectronic Fabrication (2nd ed.). Upper Saddle River: Prentice Hall.

**[56]** Madou, Marc (2002). Fundamentals of Microfabrication. Boca Raton, Florida: CRC Press. p. 9.

**[57]** O.Martin, L. Avérous. Poly(lactic acid): plasticization and properties of biodegradable multiphase systems. Polymer .42(14): 6209–6219.

: